Entropic Uncertainty: Measuring Firm and Aggregate Uncertainty from the Graph Structure of Financial Statements*

Pierre Jinghong Liang
Accounting AI Research Lab
Carnegie Mellon University

Bo Sun
Darden School of Business
University of Virginia

Ziyi Yang
Accounting AI Research Lab
Carnegie Mellon University

Abstract

We introduce a class of uncertainty measures, *Entropic Uncertainty*, constructed by applying the factor-augmented stochastic-volatility estimator of Jurado et al. (2015) (JLN) to a novel input: the Shannon entropy of the directed weighted graph that double-entry bookkeeping induces on a firm's financial statements each quarter. Recast as a graph, the financial statements that aggregate uncertainty measures usually overlook become a rigorous, structurally disciplined record of the firm's internal resource allocation. By applying graph theory to firms' audited 10-Q and 10-K disclosures, the resulting bookkeeping graph captures, at the level of the firm's primary economic functions, how a firm allocates its internal resources, and the graph entropy summarizes the distribution of such within-firm resource flows. Running firm-level entropy through the JLN factor-augmented forecasting regression and Bayesian stochastic-volatility filter yields a firm-quarter measure of the conditional volatility of the unforecastable component of within-firm structural composition, which we aggregate into an aggregate *Entropic Uncertainty Index* (EUI). EUI carries incremental predictive power for firm investment, horse-racing favorably with existing uncertainty measures in both panel and time-series specifications. A structural decomposition of the bookkeeping graph entropy delivers channel-specific uncertainty readings whose differential predictive performance is itself informative. Collectively, the results establish financial-statement structure as an internally grounded, theoretically disciplined, and empirically rich source of uncertainty measurement.

Keywords: Uncertainty; entropy; graph theory; financial statements; stochastic volatility; investment.

JEL Classification: D80, E32, E44, G31, M41.

*Bo Sun visited the Accounting AI Research Lab while some of this work was done. The authors are grateful for the encouragement and suggestions by lab members during these visits. Pierre Jinghong Liang is grateful for the support provided by the Marvin Goodfriend summer fellowship program of the Tepper School. Ziyi Yang is grateful for the William Larimer Mellon doctoral fellowship. The authors acknowledge financial-statement graph and entropy data provided by Liang and Pyo (2026a) of the Accounting AI Research Lab at Carnegie Mellon University's Tepper School of Business under a Data Use Agreement (DUA). Visit `https://www.cmu.edu/tepper/accounting-lab/` for more information on the lab. All interpretations are our own. Corresponding author: Pierre Jinghong Liang (liangj@andrew.cmu.edu).

1 Introduction

Uncertainty is one of the central objects of modern economics, yet most widely used uncertainty measures stand outside the firm. Market-based measures are confounded with risk premia, leverage, and sentiment; text-based measures are entangled with rhetoric, attention, and the language used to narrate events; and leading econometric measures, while conceptually disciplined, are usually built from externally observed outcomes rather than from the firm's own information-production system. This paper starts from a different premise. Before uncertainty is reflected in prices, newspapers, or surveys, it is first encoded in the internal economic organization of the firm as recorded in its financial statements.

Financial statements encode a classified map of the firm's internal allocation of economic resources. They are highly structured objects generated by double-entry bookkeeping, which links stocks and flows across the balance sheet, income statement, statement of cash flows, and statement of shareholders' equity. The algebraic structure of double-entry bookkeeping has been recognized since Pacioli and formalized by accounting theorists such as Ijiri (1975) (see also Arya et al. (2000)); what is new is the capacity to analyze that structure empirically, at scale, with the tools of modern graph theory and data mining. Its natural mathematical representation is a weighted directed graph: nodes are accounts, edges are consolidated journal entries, and edge weights are the dollar amounts that flowed between accounts during the quarter. The financial-statement graph therefore provides a compact and economically rich representation of the firm's internal resource-allocation system.

We construct our entropic uncertainty measures from the graph-theoretic structure of the firm's own financial statements, specifically from the Shannon entropy applied to the weighted directed graph that double-entry bookkeeping induces on the firm's quarterly financial statement filings (following the pioneering use of Shannon entropy on firm-level balance-sheet and income-statement composition by Theil (1969)). The graph is an object of the firm's own audited record, constrained by three universal bookkeeping laws (balance, conservation, and linear aggregation), and visible to outside observers through the 10-Q/10-K filings that Generally Accepted Accounting Principles (GAAP) require. Its Shannon entropy—by the axiomatic derivation of Shannon (1948)—is the unique summary of the edge-share distribution satisfying continuity, monotonicity, and additive decomposition under refinement (Cover and Thomas, 2006; Liang, 2026)).

Since Coase (1937), economists have understood the firm as an institution defined by the internal allocation of economic resources: a domain in which non-market governance allocates resources in lieu of the price mechanism (Williamson, 1985; Grossman and Hart, 1986; Hart and Moore, 1990; Holmström and Milgrom, 1991). The firm exists, in this tradition, because such internal allocation is the firm's economic content; markets handle external exchange, and firms handle the structured internal flows that production, financing, and value creation require. How firms reallocate resources internally, in turn, should be a first-order determinant of firm-level and aggregate performance.[1] Despite the centrality of internal reallocation, a firm-level, period-by-period measure has been unavailable. We construct such a measure and show that it provides a window into the uncertainty firms face.

What graph and its entropy represents. The object we work with is unfamiliar to most economists, and we introduce it before deriving its entropy. Under double-entry bookkeeping, every transaction a firm undertakes is recorded as a debit to one account and an offsetting credit to another, for the same dollar amount. By the standard journal-entry convention adopted in Liang (2026), an edge $e = (c, d) \in \mathcal{E}_{it}$ is directed from the credited account c to the debited account d, with weight $w_{it}(e)$ equal to the dollar amount of the entry. A quarter of firm activity therefore generates a collection of triples (debit account, credit account, dollar amount), which is mathematically a weighted directed graph: accounts are nodes, journal entries are edges, dollar amounts are edge weights. The four primary statements—balance sheet, income statement, statement of cash flows, and statement of shareholders' equity—are joint projections of this graph, linked by three universal bookkeeping laws (balance, conservation, and linear aggregation) that constrain admissible graphs to a structured manifold (Ijiri, 1975; Arya et al., 2000; Liang, 2026). The graph is, in this sense, a structural primitive of the firm's own economic record: it summarizes *which* channels carried *how much* of the quarter's activity, with the consistency discipline that auditing imposes. The financial-statement graph is the intra-firm analogue to graph-application in production networks (Acemoglu et al., 2012; Herskovic, 2018): it is a period-by-period map of how economic resources moved within the firm's boundaries.

The Shannon entropy H of the edge-weight distribution is a scalar summary of how the quarter's economic activity is distributed across this graph's channels. A firm that concentrates transaction volume on a few edges has low H; a firm whose activity spreads across many edges of comparable magnitude has high H. The mapping is the same one economists know from industrial organization, where Shannon entropy is the information-theoretic counterpart of the Herfindahl–Hirschman index: low entropy corresponds to concentration, high entropy to dispersion.[2] Economically, H measures the *effective dimensionality* of the firm's current internal economic configuration as seen through the GAAP lens. It is a structural state at a point in time, summarizing the distribution of a firm's internal resource composition.

This entropy-measured state is thus an equilibrium object: Each edge of the graph is the realized outcome of an optimization: working-capital, investing, financing, pricing, and payout policies,

[1] A large empirical literature has documented that the allocation of resources matters, both *between* firms—through cross-firm dispersion in marginal revenue products of capital and labor (Hsieh and Klenow, 2009; David and Venkateswaran, 2019)—and *within* firms—through cross-divisional capital allocation in conglomerates (Lamont, 1997; Stein, 1997).

[2] Formally, $\exp(H)$ is the *effective number* of edges (the perplexity), the Shannon-entropy counterpart of the inverse-HHI "effective number of competitors" in industrial organization (Adelman, 1969). Both are "effective number" summaries of a share distribution; they coincide when shares are uniform but in general weight rare and common components differently.

chosen by the firm given its information, applied to an unobserved economic state that encompasses demand, input costs, financing conditions, and the policy environment. Graph entropy thus inherits two sources of variation: deliberate firm response to anticipated conditions, and unanticipated state realizations that force unplanned adjustment. The JLN factor-augmented forecasting regression in Section 4.1 exploits this structure: it removes the predictable component, leaving a residual whose conditional volatility is—under the same rational-expectations logic that justifies reading profit-growth as uncertainty in Jurado et al. (2015)—an internal, ledger-based reading of the time-varying uncertainty in the firm's economic environment.

Why graph entropy is a useful input for an uncertainty filter. The firm's structural state at t, as encoded in its bookkeeping graph, is a distribution: the edge-share vector π_{it} over the channels through which the quarter's economic activity flowed. Any filter that purports to extract uncertainty about this state must first reduce the distribution to a scalar summary. By the axiomatic derivation of Shannon (1948), Shannon entropy is the unique scalar functional of a distribution that is continuous, increasing under equiprobability, and additively decomposable across coarse-fine partitions.[3] Entropy is, in this sense, the only scalar of π_{it} whose movements a filter can interpret without reference to an arbitrary aggregation rule, and whose decomposition across operating, income-statement, and financing subgraphs inherits the same axiomatic discipline.[4]

The graph entropy is a state, not a flow, and this distinction shapes what its filtered conditional volatility measures. The graph entropy summarizes the configuration the firm is in at t, the accumulated outcome of all past decisions and shocks, and its movement from $t-1$ to t records the structural reorganization the firm has undertaken in response to the conditions it faces. The conditional volatility of this state, after the predictable component is removed, therefore measures uncertainty about *how the firm is configured*—a margin to which the adjustment-cost and irreversibility frictions of Bernanke (1983) and Dixit and Pindyck (1994) attach, since those frictions are precisely what make configuration sticky and costly to undo. Irreversibility frictions operate on structural margins: capital stocks, organizational arrangements, contractual commitments. The bookkeeping graph records such structural margins (asset composition, working-capital deployment, financing structure). State- uncertainty and flow-uncertainty are conceptually distinct objects, and in the empirical horse races we find that they are empirically distinct as well: filtered structural-state volatility carries predictive content for investment beyond filtered profit-growth volatility, and the predictive content is sharpest for the operating subgraph—the subgraph that contains the investing- cash-flow edge through which capital irreversibility operates directly.

Several properties of the input class follow. The measure is internal to the firm: read from

[3] Alternative summaries—the Herfindahl index, the Gini coefficient, the maximum share—each violate at least one of these properties, and in particular the failure of additive decomposition under refinement makes them unsuitable for the subgraph attribution that the bookkeeping structure naturally permits.

[4] Information-theoretic functionals are the operational primitives by which uncertainty has been formalized in macroeconomics for two decades. See Section 3.1 for a discussion of the literature on uncertainty measurement and the robust-control framework of Hansen and Sargent (2008),

audited disclosures rather than from market prices, analyst forecasts, surveys, or text, it is insulated from the contamination channels—risk premia, sentiment, rhetoric, reporting incentives—that burden expression- and valuation-based proxies. It is GAAP-disciplined: the graph is the mathematical structure that audited disclosures generate, and the bookkeeping laws restrict admissible graphs to a structured manifold, so that variation in H_{it} is variation in a constrained, well-defined object. And it is decomposable by economic activity: the subgraph partition of Liang et al. (2026) yields separate filtered volatilities for operating, income-statement, and financing channels, isolating economic margins of uncertainty.

Implementation. We adopt the Jurado et al. (2015) estimator without modification. The choice is deliberate: by using the same two-stage factor-augmented stochastic-volatility procedure on the same panel of macro and financial factors, any difference between Entropic Uncertainty and the firm-level profit-based uncertainty of Jurado et al. (2015) is attributable to the input series rather than to the filter. Stage 1 projects firm-quarter graph entropy on its own lags, on principal components extracted from the cross-firm panel of entropy series, on the JLN macro and financial factors, and on standard firm controls; selection of lags and factors follows JLN's hard-thresholding rule. Stage 2 models the Stage 1 residual as a log-linear AR(1) stochastic-volatility process estimated by the ancillarity-sufficiency-interweaving MCMC of Kastner and Frühwirth-Schnatter (2014), with multi-step uncertainties at horizons $h = 1 - 4$ obtained by the JLN recursion. Firm-level Entropic Uncertainty is the posterior mean of the conditional volatility; the aggregate Entropic Uncertainty Index (EUI) is the cross-firm average. We construct the measure from two inputs in parallel: the entropy of the full bookkeeping graph H^{Tot} and the entropy of its operating subgraph H^{OG}. The conceptual framework above identifies the operating subgraph—the partition containing the working-capital and investing-cash-flow edges—as the structural margin to which capital-adjustment frictions attach most directly, and the empirical results bear out the prediction that this subgraph yields the clearest reading.

Findings. We assess our uncertainty measures through three exercises that escalate in the demands they place on it. The first is comovement with external aggregate uncertainty benchmarks. The Entropic Uncertainty Index tracks JLN Macro and JLN Financial uncertainty, the EPU index of Baker et al. (2016), and the VIX. The comovement is strong enough to confirm that EUI is informative about fluctuations in uncertainty, though EUI retains independent variation.

The second exercise asks whether Entropic Uncertainty captures firm-specific uncertainty that markets price contemporaneously. At the firm-quarter level, Entropic Uncertainty is associated with idiosyncratic stock-return volatility—the residual volatility from market-model regressions, the standard market-based proxy for firm-level uncertainty—both in time series and in panel regressions, and the association survives the inclusion of profit- based JLN, EPU, VIX, and JLN Macro and Financial as controls. That is, our measure built entirely from audited disclosures, using no market data, lines up with the firm-specific risk that equity markets price.

The third exercise is on the predictive content for the real economic decision that uncertainty effects operate through. In firm-level panel regressions of capital investment one to four quarters ahead, Entropic Uncertainty enters significantly, with coefficient magnitudes that exceed firm-level profit-based measures, and that horse races favorably against profit-based JLN, EPU, VIX, JLN Macro, and JLN Financial jointly. The operating-subgraph variant delivers the strongest statistical result.[5] That the operating subgraph—the partition to which capital-adjustment frictions attach most directly—is the one delivering the strongest predictive performance is the empirical counterpart of the theoretical argument above: state- uncertainty along the within-firm internal fund allocation is the uncertainty most informative for investment.

Entropic Uncertainty has incremental predictive power beyond profit-based JLN is notable precisely because we use the same filter, same conditioning factors, same balanced panel as JLN. The only difference is the input class, from a line-item, flow variable of firm outcome (profit growth) to a state variable (entropy) summarizing the structural composition. The horse-race coefficient gauges the extent to which uncertainty revealed from the firm's structural configuration contributes beyond uncertainty measured from a single flow outcome.

Contribution. The paper's primary contribution is to the literature on the measurement of economic uncertainty (Bloom, 2009, 2014; Jurado et al., 2015; Baker et al., 2016; Ludvigson et al., 2021; Berger et al., 2020; Bloom et al., 2018; Cascaldi-Garcia et al., 2023). The existing literature has made substantial progress in measuring uncertainty and reads uncertainty from an extended catalog of input classes: realized and option-implied volatility of asset prices, dispersion of survey forecasts, prevalence of uncertainty-coded language in news text, and conditional volatility of macroeconomic and firm-level outcome variables. We introduce a class of input that is qualitatively different: The entropy from the graph structure in financial statements characterizes the distribution of *within-firm resource allocation*, and it is read directly from audited disclosures and is therefore insulated from potential conflating factors that may be present in market-, survey-, and text-based measurement. The horse-race results establish that this input class carries predictive content for real activity that is not subsumed by any of the conventional classes.

Additionally, because the financial-statement graph partitions into operating, income-statement, and financing subgraphs and because Shannon entropy decomposes additively under refinement, filtered uncertainty inherits the partition: the construction delivers a vector of channel-specific uncertainty readings whose joint pattern carries additional information. The operating partition is the margin to which capital-adjustment frictions attach in the irreversibility tradition (Bernanke, 1983; McDonald and Siegel, 1986; Dixit and Pindyck, 1994; Abel and Eberly, 1996; Leahy and Whited, 1996; Bloom et al., 2007; Gulen and Ion, 2016; Kim and Kung, 2017), and it is also the partition that contains the investing-cash-flow edge through which capital expenditure

[5] In one-quarter-lag firm-level panel horse races, its coefficient is substantial compared to that of the profit-JLN coefficient and other uncertainty measures. In aggregate time-series regressions of investment on uncertainty, the operating-subgraph index achieves R^2 above 0.7 and t-statistics above ten in the univariate specification, absorbing EPU and VIX in the full horse race.

literally flows. Its filtered conditional volatility is, accordingly, the sharpest predictor of future investment in the panel and dominates other uncertainty measures in the horse race. In the data, the operating-subgraph and income-statement-subgraph entropy each achieve higher aggregate R^2 in investment regressions than the total-graph EUI, the operating-subgraph entropy comoves strongly with idiosyncratic stock return volatility. The differential pattern across channels admits a margin-aligned reading of where uncertainty operates on real activity.

2 Financial-Statement Graphs and Graph Entropy

In this section we introduce the graph-theory application on financial-statements, following Liang et al. (2026). We show how double-entry bookkeeping—the universal recording system underlying audited financial disclosures worldwide—generates a weighted directed graph as its mathematical object, how the three bookkeeping laws constrain admissible graphs to a structured manifold, and how the firm's published 10-Q and 10-K disclosures permit the recovery of this graph at quarterly frequency. The construction is the machinery developed in Liang et al. (2026); we present it here in an accessible form for completeness and emphasize the features that make the resulting object a disciplined input for the JLN filter.

2.1 From transactions to a graph

Under double-entry bookkeeping, every transaction the firm undertakes is recorded as a pair of equal and opposite entries: a debit to one account and a credit to another, for the same dollar amount. A quarter of firm activity therefore generates a finite collection of triples (d, c, w) where $d \in \mathcal{V}$ is the debited account, $c \in \mathcal{V}$ is the credited account, and $w \in \mathbb{R}_+$ is the dollar amount. Aggregating triples that share the same (d, c) pair yields a weighted directed graph $G_{it} = (\mathcal{V}, \mathcal{E}_{it}, w_{it})$ as in Definition 1: nodes are accounts, edges are aggregated journal entries, and edge weights are the total dollar volumes that flowed between each pair of accounts during the quarter. The graph is the firm's activity, in the form the firm itself records under GAAP.

Definition 1 (Bookkeeping graph)**.** For firm i and quarter t, the bookkeeping graph is the weighted directed graph $G_{it} = (\mathcal{V}, \mathcal{E}_{it}, w_{it})$, where $\mathcal{V}$ is the set of accounts (the nodes), $\mathcal{E}_{it} \subseteq \mathcal{V} \times \mathcal{V}$ is the set of directed edges (aggregated journal entries from quarter t), and $w_{it} : \mathcal{E}_{it} \to \mathbb{R}_+$ assigns to each edge $e \in \mathcal{E}_{it}$ the dollar weight $w_{it}(e)$ (the total transaction volume between the two accounts during the quarter). Each account $v \in \mathcal{V}$ further carries a *node value* $x_{it}^{(v)} \in \mathbb{R}$, its end-of-quarter dollar balance signed by accounting convention (assets positive, liabilities and equity negative), with $\Delta x_{it}^{(v)}$ denoting its change over the quarter.

Figure 1 illustrates the construction with three transactions on the simplest possible firm: a financing-only quarter in which the firm issues common stock, takes a loan, and invests cash in a long-term securities account. The three transactions generate four nodes (the affected accounts) and three edges (the journal entries), with edge weights equal to the transaction amounts and edge directions following the credit-to-debit convention. The graph captures, in this minimal example, the same structural information that the firm's balance sheet would report—and it is this same construction, applied to a quarter of activity at a real public firm, that yields the bookkeeping graphs we work with empirically.

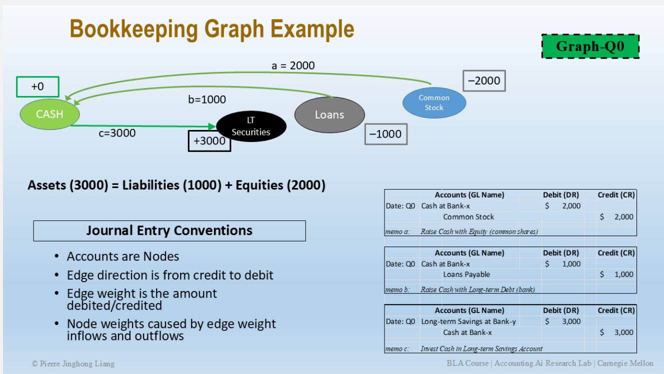

Figure 1: Bookkeeping graph: a three-transaction example. A financing-only firm in Q0 records three journal entries (lower-right panel): a \$2,000 stock issuance, a \$1,000 loan, and a \$3,000 deposit into long-term securities. Accounts are nodes, journal entries are directed edges, edge weights are transaction amounts; node weights follow from the conservation law. Construction follows Liang et al. (2026).

Three universal laws govern admissible bookkeeping graphs. Each is familiar to readers of conventional financial statements, and each can be written as an exact restriction on the graph G_{it}.

The *balance law* requires that, at every point in time, the node values sum to zero:

$$\sum_{v \in \mathcal{V}} x_{it}^{(v)} = 0, \qquad (1)$$

This is the familiar $A = L + E$ identity in graph form.

The *conservation law* requires that, for each account, the change in balance over the quarter equals the sum of inflows minus the sum of outflows along the account's edges:

$$\Delta x_{it}^{(v)} = \sum_{e:\, c(e)=v} w_{it}(e) - \sum_{e:\, d(e)=v} w_{it}(e), \qquad \text{for every } v \in \mathcal{V}, \qquad (2)$$

where $c(e)$ and $d(e)$ denote the credit (origin) and debit (destination) nodes of edge e. This is the standard T-account identity, written graph-theoretically.

The *linear-aggregation law* requires that an aggregate account formed by combining a subset $\mathcal{V}^* \subseteq \mathcal{V}$ of disaggregated accounts has balance and balance change equal to the linear sum of those of the disaggregated accounts, with weights independent of the realized values:

$$x_{it}^{(\mathcal{V}^*)} = \sum_{v \in \mathcal{V}^*} x_{it}^{(v)}, \qquad \Delta x_{it}^{(\mathcal{V}^*)} = \sum_{v \in \mathcal{V}^*} \Delta x_{it}^{(v)}. \qquad (3)$$

This is what permits, for example, the line item "Total Operating Cash Flow" on the cash-flow statement to equal the sum of its disaggregated components.

The same linearity extends to the graph's edges. When the accounts in $\mathcal{V}^*$ are merged into a single aggregate node, the journal-entry flows incident to its members add: for any external account

$u \notin \mathcal{V}^*$, the aggregate weight between $\mathcal{V}^*$ and u in each direction is the sum of the corresponding member-edge weights, $\sum_{v \in \mathcal{V}^*} w_{it}(v \to u)$, while flows internal to $\mathcal{V}^*$ net out—the graph analogue of intercompany elimination in consolidated reporting. Because the incident weights add, the conservation law (2) continues to hold at the merged node, so the linear-aggregation law (3) is a property of the whole weighted graph, not of node balances alone. Appendix A formalizes this node-merge operation.

The three laws are not assumptions we impose; they are the structural properties that auditing under GAAP enforces, and together they restrict admissible graphs to a manifold whose dimension is strictly smaller than the unrestricted space of weighted directed graphs on $|\mathcal{V}|$ nodes. The economic content is that the graph is a *closed accounting system*: every dollar of activity is recorded twice, every account balance evolves consistently with the flows in and out of it, and every aggregation preserves additive structure. The closure has two consequences for our construction. First, π_{it}, the normalized edge-share distribution introduced in Section 3.1, is a distribution on a constrained support, and its entropy $H_{it} = H(\pi_{it})$ is therefore a summary of a structured object. Second, variation in H_{it} across firms or across time is variation in a manner disciplined by these laws: it cannot reflect an idiosyncratic recording convention or an unbalanced ledger.

2.2 Recovery from public disclosures

The transaction-level graph is internal to the firm and not publicly observable. The four primary financial statements published in 10-Q and 10-K filings—balance sheet, income statement, statement of cash flows, and statement of shareholders' equity—are, however, joint projections of this graph: each statement reports a different aggregation of the underlying journal entries. Liang et al. (2026) show that the three bookkeeping laws permit the recovery of an aggregated bookkeeping graph from these articulated statements. The construction is exact at the level of the major aggregate accounts—cash flows from operations (CFO), investing (CFI), and financing (CFF); net non-cash assets (NNCA); contributed equity (CE); dividends (Div); other comprehensive income (OCI); and the income-statement components (Rev, Exp, Int. Tax)—and the resulting graph contains all the structural information that the four-statement projection retains.

We adopt this construction directly. The nodes of G_{it} are the aggregate accounts listed above; the edges are the aggregated journal-entry flows recovered by applying the three laws to the articulated statements; and the edge weights are the resulting dollar volumes. For all subsequent analysis, G_{it} refers to the firm-quarter graph constructed in this manner from Compustat quarterly fundamentals.

As an illustration, Figure 2 displays the bookkeeping graph for Walmart's fiscal year 2014–2015, constructed from the 10-K disclosures by the procedure of Section 2.2. The figure makes the abstract construction concrete: each node is an aggregate account, each directed edge is a recovered journal-entry flow, and each edge weight (in millions of dollars) is the aggregated transaction volume between the two accounts during the year. Flows between the same pair of accounts in opposite

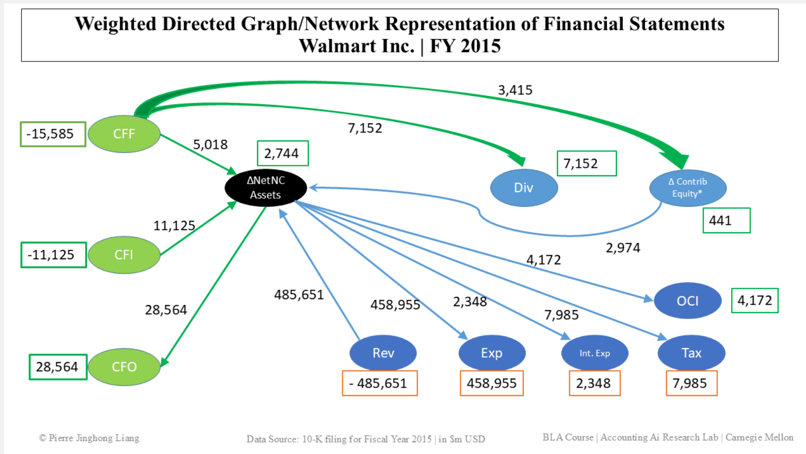

Figure 2: Financial-statement graph, Walmart, FY2014–2015. Nodes are aggregate accounts; edge weights ($M) are recovered journal-entry flows. Dashed rectangles mark the three subgraphs; H^{Tot} is the edge-share entropy and H^{OG} its operating-subgraph restriction. Media credit Liang (2026).

directions are netted into a single directed edge in this exhibit. The dashed rectangles indicate the three subgraphs developed formally in Section 2.3 below.

This firm-year graph is one of approximately 9,300 firm-quarter graphs in our estimation panel. For each, we compute H_{it}^{Tot} from the full edge-share distribution and H_{it}^{OG} from the operating-subgraph edge-share distribution; both inputs are then run through the JLN pipeline of Section 4.1.

2.3 Subgraph partition

The financial-statement graph admits an exact partition into three subgraphs corresponding to the firm's three primary economic activities. The *operating subgraph* (OG) contains the edges linking CFO, CFI, and ΔNNCA: the working-capital flows (CFO–ΔNNCA) and the investing-cash-flow channel (CFI–ΔNNCA) through which the firm deploys cash into short-term and long-term operating assets. The *income-statement subgraph* (IS) contains the edges linking the income-statement nodes (revenue, expense, interest expense, tax) to ΔNNCA and to other comprehensive income (OCI), recording the period's value-creation flows. The *financing subgraph* (FG) contains the edges linking CFF, ΔEquity, and Dividends, recording the firm's interactions with capital markets. The partition is exact: every edge of G_{it} belongs to one and only one of the three subgraphs.

Although the operating subgraph links only three nodes, edge direction makes it richer than it appears: each of its two channels (CFO–ΔNNCA and CFI–ΔNNCA) admits flows in both directions, so the subgraph can carry up to four distinct directed edges. Conceptually the bookkeeping graph is a directed multi-graph in which both directions between a pair of accounts may be nonzero; the present sample—including the Walmart and NVIDIA exhibits—nets opposing flows into a single directed edge, and richer multi-graph samples are left to future work.

As an illustration, Figure 3 displays the bookkeeping graph for NVIDIA Corporation's fiscal year ended January 31, 2023, constructed from the firm's audited 10-K disclosures by the procedure of Liang et al. (2026). The figure makes the abstract construction concrete: each node is an aggregate account, each directed edge is a recovered journal-entry flow, and each edge weight (in millions of dollars) is the aggregated transaction volume between the two accounts during the year. The colored frames indicate the three subgraphs we develop formally in Section 2.3 below: *operating* (orange, containing the CFO and CFI flows into net non-cash assets), *financing* (green, containing CFF, contributed equity, and dividends), and *income statement* (blue, containing revenue, expense, interest expense, and tax flows through net non-cash assets and other comprehensive income).

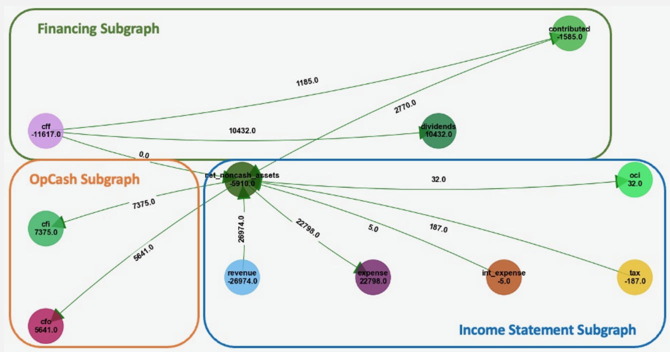

Figure 3: Bookkeeping graph: NVIDIA Corporation, FY ended Jan 31, 2023. Nodes are aggregate accounts; edge weights ($M) are journal-entry flows recovered from the 10-K via the three bookkeeping laws (1)–(3). Colored frames mark the operating (orange), financing (green), and income-statement (blue) subgraphs, formalized in Section 2.3. Entropies of the full and per-subgraph edge shares give H_{it}^{Tot}, H_{it}^{OG}, H_{it}^{FG}, and H_{it}^{IS}. Source: Liang et al. (2026).

This firm-year graph is one of approximately 9,300 firm-quarter graphs in our estimation panel. For each, we compute H_{it}^{Tot} from the full edge-share distribution and H_{it}^{OG}, H_{it}^{IS}, and H_{it}^{FG} from each subgraph's edge-share distribution; all four inputs are then run through the JLN pipeline of Section 4.1.

The partition has direct economic content. Each subgraph corresponds to a distinct margin along which firms experience and respond to uncertainty about the economic environment, and Shannon entropy applied to each subgraph reads channel-specific structural composition. Section 2.4 formalizes the additive decomposition of H_{it} into within- and between-subgraph components (Proposition 1); here we describe the three margins.

The operating subgraph contains the investing-cash-flow edge (CFI–ΔNNCA), through which capital expenditure literally flows from cash into productive assets, and the working-capital flows (CFO–ΔNNCA) governing short-term operations. Its subgraph edge therefore captures the diffusion in within-firm internal funds allocation across uses. The construction places capital expenditure inside the operating subgraph as one of its edges; the irreversibility tradition predicts that capital-adjustment frictions bind on this margin. Theory and graph construction coincide on the same partition—a coincidence the empirical results in Section 5.2 exploit.

The income-statement subgraph records the period's value-creation flows: how the firm's demand realizations, input-cost realizations, and tax treatment compose into the quarter's income statement. Filtered conditional volatility of H_{it}^{IS} is, accordingly, a reading of uncertainty in the *value-creation margin*: the conditions governing prices, costs, and earnings as they manifest in the firm's realized profit structure. This is the margin that the literature on price-setting and demand uncertainty studies most directly (Bloom, 2009; Bloom et al., 2018).

The financing subgraph reads the third channel: the firm's interactions with capital markets through debt and equity issuance, repurchases, and payout decisions. Filtered conditional volatility of H_{it}^{FG} is a reading of uncertainty in the *financing margin*: the conditions governing the firm's access to and cost of external capital. The literature on financial frictions (Gilchrist and Zakrajšek, 2012; Bernanke and Gertler, 1989) has long argued that financing-side uncertainty operates on real activity through a channel distinct from real-side uncertainty, and the financing subgraph provides a margin-aligned reading of that channel from the firm's own ledger.

Together, the three subgraphs decompose the firm's structural state into capital-deployment, value-creation, and financing margins. A single estimator applied to the entropy of each subgraph delivers three margin-aligned uncertainty readings whose joint movement permits attribution of aggregate uncertainty fluctuations to specific economic channels in different episodes—a structured uncertainty index whose properties Section 2.4 develops formally and whose empirical content we exploit for measuring uncertainty.

2.4 Graph Entropy: Formalization

We now formalize the entropy of this graph and state its additive decomposition under the subgraph partition. Following Liang et al. (2026), we define the entropy of the bookkeeping graph by treating its edge weights as the graph information functional. Normalizing the edge weights to the share simplex,

$$\pi_{it}(e) \;=\; \frac{w_{it}(e)}{\sum_{e' \in \mathcal{E}_{it}} w_{it}(e')}, \qquad \sum_{e \in \mathcal{E}_{it}} \pi_{it}(e) = 1, \tag{4}$$

yields the *edge-share distribution* π_{it}, the proportion of the quarter's recorded activity carried by each channel.

Definition 2 (Accounting Graph Entropy, AGE)**.** The Accounting Graph Entropy of firm i in quarter t is the Shannon entropy of the edge-share distribution of its bookkeeping graph,

$$\mathrm{AGE}_{it} \;\equiv\; H(\pi_{it}) \;=\; -\sum_{e \in \mathcal{E}_{it}} \pi_{it}(e)\, \log \pi_{it}(e). \tag{5}$$

We use H_{it} as shorthand for AGE_{it} throughout the paper.

The functional form is that of Shannon (1948). AGE summarizes the edge-share distribution at a point in time.[6] The axiomatic foundation for this entropy-based AGE measure is not a straightforward application of Cover and Thomas (2006). Adapting the underlying axiomatic foundation

[6] Definition 2 is a special case of the graph-entropy class introduced by Mowshowitz (1968) and formalized by Dehmer (2008): for any graph G and any *graph information functional* $f : \mathcal{S} \to \mathbb{R}_+$ on a set $\mathcal{S}$ of graph invariants,

to our bookkeeping graph edges case, we show this measure is the only edge-based measure that satisfy the three axioms. The statement and proof are given in Appendix A.

Formally, let $\mathcal{W}_m^0$ denote the set of $m \times m$ non-negative matrices $W = (w_{ij})$ with zero diagonal ($w_{ii} = 0$), with total edge mass $S(W) = \sum_{i \neq j} w_{ij} > 0$ and edge-share distribution $\pi_{ij} = w_{ij}/S(W)$ for $i \neq j$. The bookkeeping graphs of Section 3.1 are instances of this construction (with W the recovered weighted adjacency matrix); Appendix A develops the formal domain and node-relabeling quotient in full.

Denote by $J_2^{\text{bin}}(x) := J_2(\pi)$ where π is the two-edge distribution with probabilities x and $1 - x$.

Axiom 1 (Normalization). $J_2^{bin}(1/2) = 1$.

Axiom 2 (Continuity). J_2^{bin} *is continuous on* $(0, 1)$.

Axiom 3 (Node-merge grouping). *For any $W \in \mathcal{W}_m^0$ and any pair $a \neq b$, the node-merge identity* (21) *holds, with a* single *binary information function J_2^{bin} appearing in all four binary-entropy roles on the right-hand side: bilateral-elimination, row-split, column-split, and the recursive base.*

Theorem 1 (Uniqueness of edge entropy). *Suppose $\{J_m\}_{m \geq 2}$ satisfies Axioms 1–3. Then for every $m \geq 2$ and every $W \in \mathcal{W}_m^0$ with $S(W) > 0$,*

$$J_m(W) \;=\; H_m^{edge}(W).$$

The level H_{it} has a direct economic interpretation. It measures the *effective dimensionality* of the firm's structural state: $\exp(H_{it})$ is the number of equally weighted edges that would generate the same entropy as the realized edge-share distribution (the perplexity, introduced by Hill, 1973). A firm whose quarterly transaction volume concentrates on a few channels has small $\exp(H_{it})$; a firm whose volume distributes broadly has large $\exp(H_{it})$. Liang et al. (2026) also define a relative-entropy companion, the Accounting Graph Entropy-Relative $\text{AGER}_{it} = \text{KL}(\pi_{it} \,\|\, \pi_{i,t-1})$, which records realized period-over-period structural change.[7] The edge-based Accounting Graph Entropy of Definition 2 is the unique scalar summary that incorporates the full edge-weight distribution under the Shannon axioms.

Subgraph decomposition. Section 2.3 partitions the bookkeeping graph as $\mathcal{E}_{it} = \bigsqcup_s \mathcal{E}_{it}^{(s)}$ with $s \in \mathcal{S} \equiv \{\text{OG}, \text{IS}, \text{FG}\}$. Let $W_{it}^{(s)} = \sum_{e \in \mathcal{E}_{it}^{(s)}} w_{it}(e)$ denote the total edge weight of subgraph s, and $\omega_{it}^{(s)} = W_{it}^{(s)} / \sum_{s'} W_{it}^{(s')}$ its share of total graph weight. Let $H_{it}^{(s)}$ denote the Shannon entropy of the edge-share distribution within subgraph s, computed on the within-subgraph normalization $\{w_{it}(e)/W_{it}^{(s)}\}_{e \in \mathcal{E}_{it}^{(s)}}$. Where it improves readability, we write the concrete-channel instances as $H_{it}^{\text{Tot}} \equiv H_{it}$, $H_{it}^{\text{OG}} \equiv H_{it}^{(\text{OG})}$, $H_{it}^{\text{IS}} \equiv H_{it}^{(\text{IS})}$, and $H_{it}^{\text{FG}} \equiv H_{it}^{(\text{FG})}$.

the corresponding graph entropy is $H(G|f) = -\sum_k [f(s_k)/\sum_{k'} f(s_{k'})] \log[f(s_k)/\sum_{k'} f(s_{k'})]$. Accounting Graph Entropy is the instance with $\mathcal{S} = \mathcal{E}_{it}$ and $f(e) = w_{it}(e)$.

[7] Other graph-entropy measures have been developed in the bookkeeping context, including the node-based Accounting Classification Entropy of Li et al. (2024) and Laplacian-spectral (von Neumann) entropies discussed in Liang (2026).

Proposition 1 (Additive subgraph decomposition; Liang et al., 2026)**.** *The Accounting Graph Entropy of the bookkeeping graph admits the exact decomposition*

$$H_{it} \;=\; H_{it}^{(\mathcal{S})} \;+\; \sum_{s\in\mathcal{S}} \omega_{it}^{(s)}\, H_{it}^{(s)}, \tag{6}$$

where $H_{it}^{(\mathcal{S})} = -\sum_{s\in\mathcal{S}} \omega_{it}^{(s)} \log \omega_{it}^{(s)}$ *is the entropy of the subgraph weight distribution.*

This is the graph-theoretic chain rule of Shannon entropy specialized to the bookkeeping graph; Liang et al. (2026) establish it for arbitrary subgraph partitions and we restate the proofs in Appendix B. The decomposition has direct economic content. The first term, $H_{it}^{(\mathcal{S})}$, summarizes the allocation of activity *across* the firm's three primary economic functions; the second term, the weighted average of within-subgraph entropies, summarizes the allocation *within* each function. Two firms can share the same total entropy while differing sharply in this within-versus-between split, and the three subgraph entropies $\{H_{it}^{(s)}\}_{s\in\mathcal{S}}$ are economically distinct objects whose joint movement carries information that the scalar aggregate H_{it} does not. For example, the operating-subgraph entropy provides a gauge for the distribution of within-firm internal funds allocation, and it is the subgraph investment responses directly operate within.

The decomposition also licenses the structured uncertainty index of Section 3.4. Applying the JLN filter of Section 4.1 to each $H_{it}^{(s)}$ separately yields three channel-specific filtered volatilities $\mathcal{U}_{it}^{H,(s)}(h)$ that, by Proposition 1, partition the same firm-level structural state into operating, income-statement, and financing components.

3 Entropy as an Uncertainty-Measurement Input

This section develops the conceptual and empirical underpinning for financial-statement entropy as an input for uncertainty management. We first interpret the firm's structural state and explain why Shannon entropy is the appropriate scalar summary of it for the purpose of uncertainty measurement. We then formalize the logic that licenses reading the filtered conditional volatility of this scalar as a measure of uncertainty about the economic environment. We characterize the subgraph decomposition of the resulting uncertainty index. We close by documenting the empirical properties that make the financial-statement entropy series an appropriate input for the JLN filter.

3.1 The firm's structural state and its scalar summary

The edge-share distribution π_{it} defined in Section 2.4 (equation (4)) is the firm's *structural state of internal resource allocation* at t: it records, in a manner disciplined by the bookkeeping laws of balance, conservation, and linear aggregation, the proportion of the quarter's economic activity that flowed through each channel. Two firms with identical revenues and identical profits can have entirely different structural states, and the same firm can hold revenues and profits roughly fixed across periods while reorganizing its π_{it} substantially. The structural state is not a number from the financial statements; it is a property of the structure the financial statements articulate about within-firm resource flow.

A filter that purports to extract uncertainty about π_{it} must first reduce it to a scalar. Different scalar functionals impose different aggregation rules across the channels of π_{it}, and only some admit the decomposition properties that a filter applied to subgraphs can inherit consistently. The Accounting Graph Entropy $H_{it} = H(\pi_{it})$ of Definition 2 is the natural choice—and, in a precise sense, the only one.

Proposition 2 (Shannon, 1948)**.** *$H(\cdot)$ is the unique functional from the percentage simplex $\Delta^{|\mathcal{E}|-1}$ to $\mathbb{R}_+$ that satisfies (i) continuity in π, (ii) monotonicity: among uniform distributions, H is increasing in $|\mathcal{E}|$, and (iii) additive decomposition: the entropy of any partition equals the entropy of the partition weights plus the weight-averaged entropy of the within-partition distributions.*

Competing scalar summaries of π_{it}—the Herfindahl index, the Gini coefficient, the maximum share, and L^p norms for $p \neq 1$—each violate at least one of the three properties. Crucially, none is additively decomposable, the property that licenses the subgraph attribution developed in Section 2. Shannon entropy is thus, in the precise sense of Theorem 1, the only edge entropy on the constrained bookkeeping graph domain. Proposition 2 supplies the classical simplex counterpart and the decomposition property used in Section 2.4.

The choice of H as the structural-state summary draws on a broader tradition in macroeconomics. In the robust-control framework of Hansen and Sargent (2008), the decision maker's uncertainty about the data-generating process is parameterized by relative entropy, and the size of the set of alternative models the agent entertains is governed by an entropy bound. Our use of Shannon entropy to summarize the firm's structural state, and of its filtered conditional volatility to read uncertainty about that state, draws on the same intellectual lineage: information-theoretic functionals are the operational primitives by which uncertainty has been formalized in macroeconomics, whether the alternatives indexed by entropy are competing models of the world or competing channels through which a firm's resources flow.[8]

3.2 An input to the uncertainty estimator

Having established the bookkeeping graph and its entropy H_{it} in Section 2, we now treat H_{it} as the firm-quarter input to the JLN factor-augmented stochastic-volatility pipeline.

The structural state π_{it} is an equilibrium object. Each edge of the bookkeeping graph is the realized outcome of an optimization problem the firm solves: working-capital, investing, financing,

[8] Because H_{it} is a function of edge shares alone, it is invariant to proportional rescaling and symmetric in the direction of change: it reads the dispersion of within-firm activity across channels, not its level or the sign of its movement — information not contained in a signed flow variable. This is a design feature: the JLN filter removes all variation in H_{it} that is forecastable from the past, including any portion driven by anticipated policy responses to anticipated conditions; the residual is, by construction, orthogonal to the past and therefore a reading of uncertainty about the economic environment.

pricing, and payout decisions, applied to an unobserved economic state that encompasses demand, input costs, financing conditions, and the policy regime. Let s_t denote this latent economic state and $\mathbf{a}_{it} = \mathbf{a}(\,\cdot\,;\theta_i)$ the firm's policy as a function of its information set $\mathcal{I}_{it}$ and firm-specific parameters θ_i. The realized graph entropy is

$$H_{it} \;=\; h(\mathbf{a}_{it},\, s_t) \;=\; h\big(\mathbf{a}\big(s_t, \mathcal{I}_{it}; \theta_i\big),\, s_t\big)\,. \tag{7}$$

This policy-mediated character is shared with every conventional firm-level uncertainty input. Profits, returns, investment rates, and forecast errors are all jointly determined by firm policy and the realized state; none is an unmediated reading of s_t. The Jurado et al. (2015) definition of uncertainty is built precisely to handle this. For any input y_{it} and information set $\mathcal{I}_t$, JLN define h-period uncertainty as the conditional standard deviation of the unforecastable component:

$$\mathcal{U}^{y}_{it}(h) \;=\; \sqrt{\mathbb{E}\Big[\big(y_{i,t+h} - \mathbb{E}[y_{i,t+h} \mid \mathcal{I}_t]\big)^2 \,\Big|\, \mathcal{I}_t\Big]}\,. \tag{8}$$

The conditioning expectation removes whatever portion of $y_{i,t+h}$ is predictable from $\mathcal{I}_t$, including any portion driven by anticipated firm policy responses to anticipated conditions; the residual is, by construction, orthogonal to $\mathcal{I}_t$.

We take $y_{it} = H_{it}$ and implement (8) via the JLN two-stage estimator. Stage 1 projects H_{it} on a rich conditioning set: lags of H_{it} itself, principal components extracted from the cross-firm panel of entropy series, the JLN macro and financial factors, and standard firm-level controls. Denote the resulting fitted value by $\mathbb{E}[H_{it} \mid \mathcal{I}^{\text{econ}}_{t-1}]$, and the residual by $\varepsilon_{it} = H_{it} - \mathbb{E}[H_{it} \mid \mathcal{I}^{\text{econ}}_{t-1}]$.

Proposition 3. *Under the rational-expectations assumption that $\mathcal{I}^{econ}_{t-1} \subseteq \mathcal{I}_{i,t-1}$—the firm's information set is at least as rich as the econometrician's—and under standard regularity conditions on $h(\cdot,\cdot)$ and $\mathbf{a}(\cdot)$, the Stage 1 residual ε_{it} satisfies*

$$\varepsilon_{it} \;=\; h(\mathbf{a}(s_t, \mathcal{I}_{it}; \theta_i),\, s_t) \;-\; \mathbb{E}\Big[\, h(\mathbf{a}(s_t, \mathcal{I}_{it}; \theta_i),\, s_t) \;\Big|\; \mathcal{I}^{econ}_{t-1}\Big]\,, \tag{9}$$

and is driven by realizations of s_t that were not forecastable as of $t-1$. The conditional volatility $\sigma_{it} = \mathrm{Var}(\varepsilon_{it} \mid \mathcal{I}^{econ}_{t-1})^{1/2}$ inherits the scale of these unforecastable state realizations, modulated by firm-specific responsiveness θ_i.

The proposition is the formal statement of the logic that licenses JLN's firm-level profit-based measure: profits are policy-mediated, yet their post-filter innovation volatility is a reading of firm-level uncertainty because optimal policy responds to predictable variation, leaving unpredictable variation as the residual signal. Entropic Uncertainty $\mathcal{U}^{H}_{it}(h) = \hat{\sigma}_{it}(h)$ is the same construction applied to a different input: the conditional volatility of the unforecastable component of the firm's structural state, and, under Proposition 3, an internal, ledger-based reading of the time-varying uncertainty in the economic conditions the firm is navigating. The Stage 2 stochastic-volatility filter (Kastner and Frühwirth-Schnatter, 2014) estimates σ_{it} from ε_{it}; multi-step uncertainties at

$h > 1$ are obtained by the JLN recursion.

Three features of this construction warrant emphasis. First, deliberate, anticipatable policy choices—reorganizations undertaken in response to predictable shifts in conditions—are absorbed into the Stage 1 conditional mean and removed before the volatility is estimated; what remains is by construction orthogonal to forecastable action. Second, the measure is a decision-revealed one rather than expressed or priced: option-implied volatility prices expected uncertainty through derivatives markets, text-based indices quantify expressed uncertainty in discourse, and survey-based dispersion measures record stated forecast disagreement, while Entropic Uncertainty is read from the firm's realized, audited economic activity itself. Third, the measure is structured: the subgraph partition of G_{it} induces a corresponding partition of $\mathcal{U}^H$ into channel-specific components.

3.3 Distinction from existing measurement

The conceptual contribution of the construction is a distinction between two qualitatively different uncertainty objects, both recoverable from (8) but corresponding to different input classes. Conventional firm-level uncertainty inputs—profit growth, return volatility, sales growth, forecast errors—are flows: they are period-t realizations whose magnitude is mechanically tied to period-t shocks. The conditional volatility of a flow input is a reading of uncertainty about *the magnitude of contemporaneous arrivals*: how big the shock to revenues is this quarter, how large the change in profits.

Graph entropy is different. The structural state π_{it} is the configuration the firm is in at t, the accumulated outcome of all past decisions and shocks, and its movement from $t-1$ to t records the structural reorganization the firm has undertaken in response to the conditions it faces. The conditional volatility of H_{it}, after the predictable component is removed, is therefore a reading of uncertainty about *how the firm is configured*—a structural margin to which the adjustment-cost and irreversibility frictions of Bernanke (1983) and Dixit and Pindyck (1994) attach, since those frictions are precisely what make configuration slow to undo and therefore informative when it changes.

The distinction also operates along a second dimension. Profit growth is a single line-item flow extracted from the income statement; it records one number from one of the four primary statements. The edge-share distribution π_{it}, by contrast, is a characterization of the firm's full structural composition across all transaction channels: operating, investing, financing, income-statement. Its entropy H_{it} is a scalar summary of this entire distribution, not a single realization drawn from one component of it. The contrast with profit-based JLN is thus simultaneously temporal (flow versus state) and compositional (single line-item versus full structural composition). The empirical horse races in 5.2 document that this distinction is quantitatively material: filtered H-volatility carries predictive content for investment beyond filtered profit-growth volatility, in the same panel, with the same filter, and with the same conditioning factors.

3.4 Structure decomposition

The financial-statement graph admits an exact partition into operating, income-statement, and financing subgraphs (Liang et al., 2026). By the additive decomposition property of Shannon entropy (Proposition 2, item iii; Proposition 1),

$$H_{it} \;=\; \sum_{s\in\{\mathrm{OG,IS,FG}\}} \omega_{it}^{(s)}\, H_{it}^{(s)} \;+\; H_{it}^{(\mathrm{Sub})}, \tag{10}$$

where $\omega_{it}^{(s)}$ is the share of total edge weight in subgraph s, $H_{it}^{(s)}$ is the entropy of subgraph s's edge-share distribution, and $H_{it}^{(\mathrm{Sub})}$ is the entropy of the subgraph weights. Equation (10) is not a property of our construction; it is a property of Shannon entropy applied to a partitioned distribution. Applying the JLN filter to each subgraph entropy yields channel-specific uncertainty measures $\mathcal{U}_{it}^{H,(s)}(h)$ for $s \in \{\mathrm{OG, IS, FG}\}$. The aggregate $\mathcal{U}_{it}^{H}$ and the channel-specific $\mathcal{U}_{it}^{H,(s)}$ are obtained from a common estimator and a common conditioning set; they differ only in the input.

The structured character of the resulting uncertainty index is new to the measurement literature. Existing aggregate uncertainty indices—VIX, EPU, JLN Macro, JLN Financial—are scalar by design: they read uncertainty from a one-dimensional input (option prices, news text, or a panel projection). Subgraph decomposability allows the construction here to deliver, from the same estimator and the same panel, a vector of uncertainty readings whose components correspond to economically meaningful channels. Among these channels, the operating subgraph—which contains the working-capital and investing-cash-flow edges—occupies a distinguished position: it is the partition to which the adjustment-cost and irreversibility frictions of the investment-under-uncertainty literature attach most directly, and it is also the partition that contains the investing-cash-flow edge through which capital expenditure flows.

3.5 Empirical Properties of Financial-Statement Entropy

We acquire the entropy panel (firm-quarter information-theoretic summaries of the GAAP bookkeeping graph) from the Accounting AI Research Lab at Carnegie Mellon University.[9] In Appendix C, We document the empirical properties of financial-statement entropy and show that they make it an econometrically suitable input to the JLN pipeline.

Appendix C organizes the empirical patterns under five criteria that any input to the JLN factor-augmented stochastic-volatility estimator should satisfy: (i) *stationarity*, so that conditional volatility is well-defined; (ii) *forecastability*, so that Stage 1 has predictable variation to absorb; (iii) *business-cycle-relevant frequency content*, so that the Stage 2 stochastic-volatility innovations carry macroeconomic content; (iv) *conditional heteroskedasticity*, so that stochastic volatility is the

[9] The AGE/AGER panel was constructed by Liang and Pyo (2026a) at the Accounting AI Research Lab at Carnegie Mellon University and is distributed under a Data Use Agreement. Liang and Pyo (2026b) documents the panel; The dataset Liang and Pyo (2026a) contains the AGE and AGER measures and their additive decompositions at the yearly and quarterly frequencies.

appropriate filter; and (v) *economic interpretability*, so that filter output admits structural reading. The four entropy series satisfy each criterion, and the cross-correlation and cross-channel analyses below establish that the four readings carry distinct information.

4 Estimation, Data, and the Aggregate Uncertainty Series

The construction described above delivers a firm-quarter input series for each of three subgraphs (operating, income-statement, financing) and for the total graph: the Shannon entropy of the edge-share distribution at t, denoted $H_{it}^{(\cdot)}$. This section implements the JLN factor-augmented stochastic-volatility estimator on each of these inputs, describes the panel on which the estimator is run, and presents the resulting aggregate uncertainty series.

4.1 Estimation

We adopt the Jurado et al. (2015) two-stage estimator. We do so without modification: Holding the filter fixed across input series—and using the same panel of macro and financial conditioning factors that JLN deploy for their firm-level profit-based measure—ensures that any difference between Entropic Uncertainty and profit-based JLN, or among the three subgraph-level Entropic Uncertainty measures, is attributable to the input series rather than to the filter.

Stage 1: factor-augmented forecasting regression. For each input series y_{it}, Stage 1 specifies

$$y_{i,t+1} \;=\; \mu_i \;+\; \phi_i(L)\, y_{it} \;+\; \boldsymbol{\lambda}_i^{F\top} \hat{F}_t^F \;+\; \boldsymbol{\lambda}_i^{M\top} \hat{F}_t^M \;+\; \boldsymbol{\gamma}_i^\top W_{it} \;+\; \varepsilon_{i,t+1}, \tag{11}$$

where $\phi_i(L)$ is a lag polynomial in y_{it}; $\hat{F}_t^F$ are principal components extracted from the cross-firm panel $\{y_{jt}\}_{j=1}^N$, capturing common variation in firms' structural states; $\hat{F}_t^M$ are the JLN macro and financial factors estimated from the FRED-MD-based macro dataset (Jurado et al., 2015; Ludvigson et al., 2021); and W_{it} is a vector of firm-level controls (log total assets, leverage, firm age, industry indicators). Lag orders and factor loadings are selected by hard thresholding on t-statistics, following JLN's selection rule. The fitted value $\mathbb{E}[y_{i,t+1} \mid \mathcal{I}_t^{\text{econ}}]$ is, by Proposition 3, the component of $y_{i,t+1}$ predictable from the conditioning set; the residual $\varepsilon_{i,t+1}$ is orthogonal to it by construction and, under rational expectations, driven by state realizations s_{t+1} that were not forecastable as of t.

Stage 2: stochastic volatility. Stage 2 models the conditional volatility of the Stage 1 residual as a log-linear AR(1) stochastic-volatility process,

$$\varepsilon_{it} = \sigma_{it}\, \xi_{it}, \qquad \xi_{it} \overset{\text{iid}}{\sim} \mathcal{N}(0,1), \tag{12}$$

$$\log \sigma_{it}^2 = \alpha_i + \beta_i \log \sigma_{i,t-1}^2 + \tau_i \eta_{it}, \qquad \eta_{it} \overset{\text{iid}}{\sim} \mathcal{N}(0,1), \tag{13}$$

with $\xi_{it} \perp \eta_{it}$. The model is estimated by the ancillarity-sufficiency-interweaving MCMC of Kastner and Frühwirth-Schnatter (2014). Multi-step conditional volatilities $\sigma_{it}(h)$ for $h = 1, \ldots, 4$ are obtained by the JLN recursion, which propagates time-varying volatility through both the Stage 1 conditional mean and the Stage 2 process.

Inputs and aggregation. We run the estimator on each of the structural-state inputs introduced in Section 2: total graph entropy H_{it}^{Tot}, operating-subgraph entropy H_{it}^{OG}, income-statement subgraph entropy H_{it}^{IS}, and financing-subgraph entropy H_{it}^{FG}. Each input yields a firm-quarter conditional-volatility series, which we aggregate to the macro level by two complementary methods: the cross-sectional average (CSA) and the first principal component of the firm-level panel (PCA). For input class c and horizon h, firm-level Entropic Uncertainty is

$$\mathcal{U}_{it}^{c}(h) \;=\; \hat{\sigma}_{it}^{c}(h), \tag{14}$$

and the corresponding aggregate Entropic Uncertainty Index has CSA and PCA variants

$$\text{EUI}_t^{c,\text{CSA}}(h) \;=\; \frac{1}{N_t}\sum_{i\in\mathcal{S}_t}\mathcal{U}_{it}^{c}(h), \qquad \text{EUI}_t^{c,\text{PCA}}(h) \;=\; \text{PC}_1(\{\mathcal{U}_{it}^{c}(h)\}_{i\in\mathcal{S}_t})\,. \tag{15}$$

The CSA index treats each firm as an equal-weighted draw from the cross section; the PCA index isolates the dominant common factor across firms. We report results for both.

4.2 Data

Estimation panel. We begin with a strict overlapping sample with JLN for benchmarking considerations. We extend our sample to the present in the next section, finding consistent results.

The bookkeeping graph entropy dataset, constructed from Compustat North America quarterly fundamentals over 1990Q1–2024Q4. For the strict overlapping sample, we require each firm to have both a complete entropy series and a complete profit-growth series in every quarter. The Jurado et al. (2015) firm-level estimation 1970-2011 window and the entropy data overlap for a 86-quarter window over 1990Q1–2011Q2. This balanced-panel restriction is the same one Jurado et al. (2015) impose for their firm-level profit-based measure; we adopt it to obtain an identical sample for clear benchmarking.

We use this sample as our baseline panel for clear comparison to the firm-level JLN benchmark. The balanced-panel restriction selects firms whose configurations are stable enough to survive twenty-one years of continuous quarterly disclosure—the firms whose structural-state volatility should be *smallest* in the cross-section. The estimates that follow are therefore biased against our measure: a sample drawn to favor long-run structural stability is not a sample in which the informativeness of structural-state innovations is maximized. The resulting cross section contains $N = 123$ firms over $T = 86$ quarters, yielding approximately 10,578 firm-quarter observations.

Uncertainty benchmarks. We compare Entropic Uncertainty against external benchmarks that span the principal input classes of the existing measurement literature: VIX (asset-price input); EPU (Baker et al., 2016) (text input); JLN Macro and JLN Financial (Jurado et al., 2015; Ludvigson et al., 2021) (panel-projection inputs applied to FRED-MD-based macro and financial outcomes); and firm-level profit-based JLN, the closest methodological cousin of our measure. All measures are at horizon $h = 1$, sampled or averaged to quarterly frequency, and standardized within the window to facilitate comparisons in the regression tables.

Outcome variables. The principal downstream outcome variable is capital investment, measured as CAPX divided by beginning-of-period total assets, evaluated at horizons $h \in \{1, 2, 3, 4\}$ ahead of t. For the firm-level association exercise of Section 5.1, we additionally use idiosyncratic stock-return volatility, computed as the standard deviation of daily residuals from a market-model regression within each firm-quarter.

Inference. Firm-level panel regressions include firm fixed effects throughout, with time fixed effects added in specifications that include only firm-varying regressors and dropped in specifications that include purely time-series benchmarks. Standard errors are clustered by firm. Aggregate time-series regressions are estimated by OLS on cross-sectional means with Newey–West standard errors.

4.3 The Aggregate Entropic Uncertainty Series

We now turn to the aggregate uncertainty series the construction delivers. The panel of firm-level filtered volatilities, aggregated to either CSA or PCA, produces a family of Entropic Uncertainty indices, indexed by input class and horizon. Before considering their predictive content for downstream firm decisions, it is useful to characterize the series themselves: what the underlying structural-state series look like, what their filtered uncertainty counterparts look like, and how the two aggregation schemes compare.

Each firm-quarter input series is run through the JLN two-stage estimator and aggregated to the macro level under both CSA and PCA schemes. The resulting aggregate Entropic Uncertainty Indices are economically and statistically informative in their own right, and we examine them here before turning to predictive regressions.

Aggregate Entropic Uncertainty Indices and external benchmarks. Figure 4 plots the Total Graph and Operating-Subgraph Entropic Uncertainty Indices alongside JLN Macro, JLN Financial, EPU, and VIX over the sample window. The series share the major business-cycle elevations—all rise during the 2001–2002 contraction and the 2007–2009 financial crisis—but diverge in detail. The Total Graph EUI registers a sharp spike in 2002 that exceeds JLN Macro and the option-implied VIX in amplitude; the Operating-Subgraph EUI carries a different signature, with sustained elevation through the mid-2000s that the conventional benchmarks do not display. The pairwise correlations between EUI and the conventional benchmarks (in the range 0.2–0.5) confirm that EUI carries a substantial component of variation not captured by the existing measurement classes.

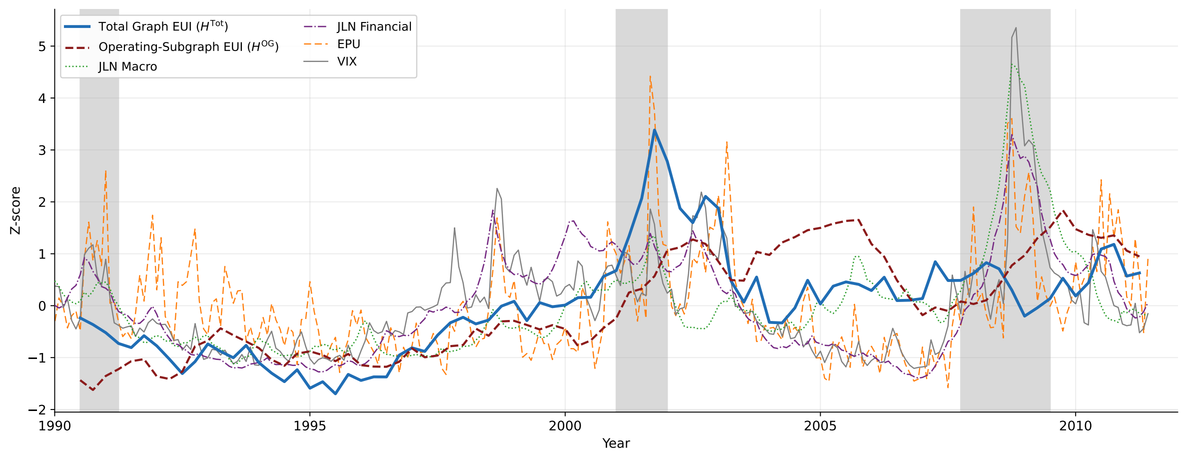

Figure 4: Entropic Uncertainty Indices and external benchmarks, 1990Q1–2011Q2. Total Graph EUI based on H^{Tot} (solid blue), Operating-Subgraph EUI based on H^{OG} (dashed dark red), JLN Macro (dotted green), JLN Financial (dash-dotted purple), EPU (long-dashed orange), and VIX (gray). All series at horizon $h = 1$, standardized to mean zero and unit variance over the sample window. Shaded vertical bands indicate NBER recessions (1990Q3–1991Q1, 2001Q1–2001Q4, 2007Q4–2009Q2).

Subgraph-level Entropic Uncertainty Indices. Figure 5 plots the four EUI series together. The four channels share business-cycle timing but differ markedly in amplitude and persistence. The 2002 episode appears as a near-synchronous peak across all four channels; by contrast, in the mid-2000s the operating-subgraph EUI rises while the financing-subgraph EUI declines, and the income-statement-subgraph EUI rises steadily through 2008–2009 to its sample peak. The distinct profiles preview the differential predictive performance documented in Section 5.2: each subgraph reads uncertainty along a structurally distinct margin, and the time-series behavior of each margin differs in a manner the scalar Total EUI cannot reveal.

CSA versus PCA aggregation. The two aggregation schemes deliver qualitatively similar series. Under CSA, each firm contributes equal weight; under PCA, each firm is weighted by its loading on the dominant common factor. We report results for both throughout. Differences are concentrated in the relative weight given to large idiosyncratic episodes: PCA dampens single-firm shocks; CSA preserves them. The qualitative pattern of the series is preserved across schemes, indicating that the aggregate signal is driven by common rather than idiosyncratic variation.

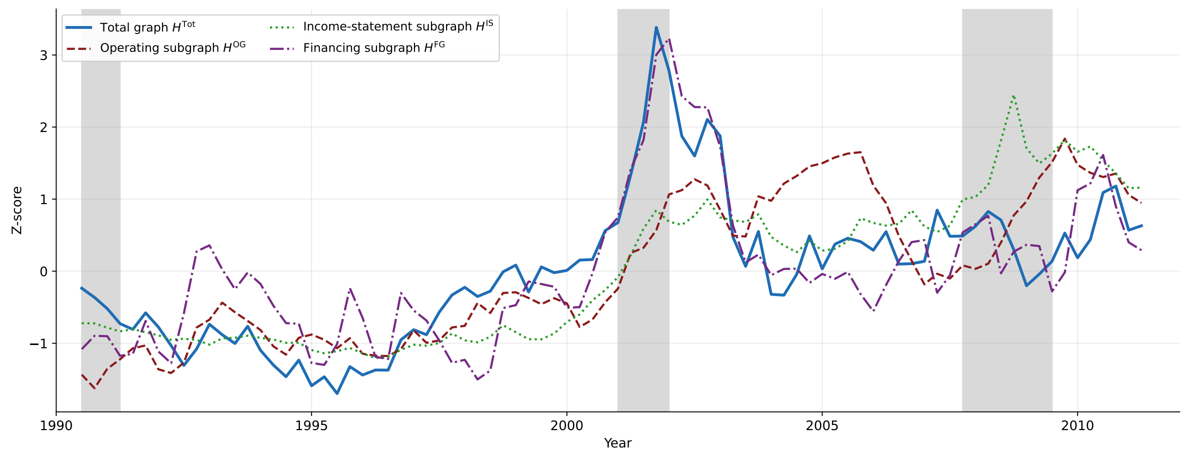

Figure 5: Subgraph-level Entropic Uncertainty Indices, 1990Q1–2011Q2. Filtered EUI series for the four Shannon-entropy inputs: total graph H^{Tot} (solid blue), operating subgraph H^{OG} (dashed dark red), income-statement subgraph H^{IS} (dotted green), and financing subgraph H^{FG} (dash-dotted purple). All series at horizon $h = 1$ under CSA aggregation. Shaded vertical bands indicate NBER recessions.

5 Evaluation of information content

This section evaluates the information content of Entropic Uncertainty. Section 5.1 examines whether the measure captures firm-specific uncertainty that equity markets price contemporaneously. Section 5.2 examines whether the measure carries incremental predictive content for the most theoretically grounded real-side decision in the firm-level uncertainty literature: capital investment. Section 5.3 discusses the channel-specific uncertainty readings the structured construction produces. While the analyses in Section 5.1 through Section 5.3 use the strict overlapping sample with JLN for benchmarking, Section 5.4 demonstrates that the results are robust in the extended sample.

5.1 Contemporaneous stock return volatility

A first test of measurement validity is whether Entropic Uncertainty comoves with market-based indicators of firm-level uncertainty. Following Alfaro et al. (2024), we use idiosyncratic stock-return volatility, the residual standard deviation from a market-model regression. The test asks whether a measure built entirely from audited disclosures, using no market data, lines up with the firm-specific risk that equity markets price. Because the structured construction delivers four channel-specific EUIs, we examine each in turn: a single-channel comovement may be informative about which margin of structural uncertainty markets actually price.

We test the hypothesis at the firm-quarter panel level using contemporaneous regressions of idiosyncratic return volatility on each EUI in turn, controlling for firm fixed effects (and time fixed effects in columns I and II) with standard errors clustered by firm.[10] Tables 1–4 report the four

[10]Time fixed effects absorb pure time-series benchmarks (EPU, VIX, JLN Macro, JLN Financial), so columns III and IV drop time fixed effects to admit these controls.

channel-specific results.

Table 1: Stock Return Volatility and EUI^{tot} — Contemporaneous Panel

	I	II	III	IV
EUI^{tot}	0.0028***	0.0021**	0.0022**	0.0014*
	(2.84)	(2.22)	(2.36)	(1.65)
JLN Firm		0.0064***	0.0073***	0.0068***
		(4.40)	(4.57)	(4.67)
EPU			−0.0033***	−0.0049***
			(−4.88)	(−7.08)
VIX			0.0208***	0.0027**
			(22.03)	(2.30)
JLN Macro				0.0075***
				(5.09)
JLN Finance				0.0173***
				(12.29)
N	9,898	9,898	9,898	9,898
R^2	0.012	0.024	0.153	0.187
Fixed Effects	Firm + Time	Firm + Time	Firm	Firm
Firm Controls		Yes		

Notes: EUI^{tot} is the total-graph Entropic Uncertainty Index (standardized). Dependent variable is contemporaneous annualized within-quarter stock return volatility ($h = 0$). Uncertainty measures standardized (mean 0, s.d. 1). t-statistics in parentheses (clustered by firm). *** $|t| \geq 2.576$; ** $|t| \geq 1.960$; * $|t| \geq 1.645$. Specs I–II include firm and time FE; Specs III–IV include firm FE only (aggregate benchmarks would be absorbed by time FE).

The operating-subgraph EUI loads positively and significantly on contemporaneous idiosyncratic return volatility at every specification (Table 2). The coefficient is robust to including JLN Firm uncertainty, to adding EPU and VIX, and to adding JLN Macro and JLN Financial; the column IV coefficient is 0.0031 with $t = 3.61$, indicating that operating-subgraph structural uncertainty loads on idiosyncratic stock return volatility incrementally to all conventional benchmarks. The income-statement-subgraph EUI loads positively but only marginally, with significance disappearing once benchmarks are added.

The differential is informative for what Entropic Uncertainty captures. Equity markets price firm-level risk that comoves with operating-margin structural uncertainty: when a firm's working-capital and investing-cash-flow deployment becomes more uncertain, its returns become more volatile in the same quarter, incrementally to all conventional benchmarks.

5.2 Predictive Content for Capital Investment

We now ask the central empirical question of the paper: does Entropic Uncertainty predict future capital investment, and does it do so incrementally to the conventional uncertainty benchmarks? The investment-under-uncertainty literature predicts that uncertainty matters for investment through capital-adjustment frictions (Bernanke, 1983; McDonald and Siegel, 1986; Dixit and

Table 2: Stock Return Volatility and EUI$^{\mathrm{OG}}$ — Contemporaneous Panel

	I	II	III	IV
EUI$^{\mathrm{OG}}$	0.0036***	0.0031***	0.0036***	0.0031***
	(4.10)	(3.74)	(3.71)	(3.61)
JLN Firm		0.0063***	0.0071***	0.0066***
		(4.53)	(4.70)	(4.77)
EPU			−0.0033***	−0.0048***
			(−4.90)	(−7.17)
VIX			0.0208***	0.0027**
			(21.99)	(2.36)
JLN Macro				0.0073***
				(5.08)
JLN Finance				0.0174***
				(12.16)
N	9,898	9,898	9,898	9,898
R^2	0.015	0.027	0.156	0.190
Fixed Effects	Firm + Time	Firm + Time	Firm	Firm
Firm Controls		Yes		

Notes: EUI$^{\mathrm{OG}}$ is the operating-subgraph Entropic Uncertainty Index (standardized). Dependent variable is contemporaneous annualized within-quarter stock return volatility ($h = 0$). Uncertainty measures standardized (mean 0, s.d. 1). t-statistics in parentheses (clustered by firm). *** $|t| \geq 2.576$; ** $|t| \geq 1.960$; * $|t| \geq 1.645$. Specs I–II include firm and time FE; Specs III–IV include firm FE only (aggregate benchmarks would be absorbed by time FE).

Pindyck, 1994; Abel and Eberly, 1996); firm-level evidence on this prediction is provided by Leahy and Whited (1996), Bloom et al. (2007), Gulen and Ion (2016), and Kim and Kung (2017). Real-options theory delivers a sharp sign prediction: higher uncertainty raises the option value of waiting and reduces realized capital expenditure. The closest measurement antecedent is firm-level profit-based JLN, with which we share the filter, the conditioning factors, and the balanced panel.

The dependent variable in all specifications is CAPX divided by beginning-of-period total assets, evaluated at horizons $h \in \{1, 2, 3, 4\}$ ahead of t. Regressors are standardized to mean zero and unit variance for cross-measure coefficient comparability. Firm-level panel regressions include firm fixed effects throughout, with time fixed effects added in specifications that include only firm-varying regressors and dropped in specifications that include purely time-series benchmarks (since the latter would be absorbed by time fixed effects). Aggregate time-series regressions are estimated by OLS on cross-sectional means with Newey–West HAC standard errors at $\max(h + 1, 4)$ lags.

We report four tables. Tables 5–6 report firm-level panel regressions with inputs H_{total} and H_{OG} respectively; Tables 7–8 report the corresponding aggregate time-series regressions. Within each table, Panels A and B vary the controls included with EUI, while Panels C and D add the pure time-series benchmarks. The progression isolates the incremental contribution of Entropic Uncertainty as additional benchmarks are introduced.

Table 3: Stock Return Volatility and $\mathrm{EUI}^{\mathrm{FG}}$ — Contemporaneous Panel

	I	II	III	IV
$\mathrm{EUI}^{\mathrm{FG}}$	−0.0002	−0.0004	−0.0003	−0.0004
	(−0.27)	(−0.57)	(−0.54)	(−0.58)
JLN Firm		0.0065***	0.0074***	0.0069***
		(4.59)	(4.74)	(4.82)
EPU			−0.0032***	−0.0048***
			(−4.77)	(−7.05)
VIX			0.0208***	0.0026**
			(21.97)	(2.24)
JLN Macro				0.0075***
				(5.05)
JLN Finance				0.0174***
				(12.33)
N	9,898	9,898	9,898	9,898
R^2	0.011	0.024	0.153	0.187
Fixed Effects	Firm + Time	Firm + Time	Firm	Firm
Firm Controls		Yes		

Notes: $\mathrm{EUI}^{\mathrm{FG}}$ is the financing-subgraph Entropic Uncertainty Index (standardized). Dependent variable is contemporaneous annualized within-quarter stock return volatility ($h = 0$). Uncertainty measures standardized (mean 0, s.d. 1). t-statistics in parentheses (clustered by firm). *** $|t| \geq 2.576$; ** $|t| \geq 1.960$; * $|t| \geq 1.645$. Specs I–II include firm and time FE; Specs III–IV include firm FE only (aggregate benchmarks would be absorbed by time FE).

Firm-Level Panel: Total Graph Entropy. Table 5 reports firm-level panel regressions with EUI constructed from H_{total}. EUI loads negatively and significantly on future investment at all four horizons in every specification, with t-statistics ranging from −2.5 to −5.6. The negative sign is exactly the sign predicted by the real-options theory of Bernanke (1983) and Dixit and Pindyck (1994): higher uncertainty raises the option value of waiting and depresses realized capital expenditure. Furthermore, in the bivariate horse race against profit-based JLN (Panel B), the EUI coefficient (−0.0005 at $h = 1$) is about a third larger than the profit-JLN coefficient (−0.0004 at $h = 1$) in the same panel and with the same filter. In the full horse race that adds EPU, VIX, JLN Macro, and JLN Financial (Panel D), EUI retains its sign and significance at $t = -5.17$ at $h = 1$, alongside JLN Macro ($t = -4.25$) and EPU ($t = -2.40$).

Firm-Level Panel: Operating-Subgraph Entropy. Table 6 repeats the firm-level panel exercise with EUI constructed from H_{OG}. The operating-subgraph variant delivers a sharper pattern than the total-graph variant. The EUI coefficient at $h = 1$ is −0.0012 in Panel A and −0.0015 in Panel D, with t-statistics ranging from −3.5 to −7.6 across specifications. In the full horse race (Panel D), the operating-subgraph coefficient (−0.0015, $t = -7.51$) is materially larger than the profit-JLN coefficient (−0.0003, $t = -1.51$) and exceeds in magnitude other firm-varying measures carrying the theoretically predicted sign.

Table 4: Stock Return Volatility and EUI^{ISG} — Contemporaneous Panel

	I	II	III	IV
EUI^{ISG}	0.0019*	0.0010	0.0022**	0.0009
	(1.91)	(0.91)	(2.00)	(0.88)
JLN Firm		0.0064***	0.0072***	0.0068***
		(4.34)	(4.45)	(4.58)
EPU			−0.0034***	−0.0049***
			(−5.04)	(−7.17)
VIX			0.0207***	0.0026**
			(21.97)	(2.27)
JLN Macro				0.0073***
				(4.82)
JLN Finance				0.0174***
				(12.33)
N	9,898	9,898	9,898	9,898
R^2	0.012	0.024	0.154	0.187
Fixed Effects	Firm + Time	Firm + Time	Firm	Firm
Firm Controls		Yes		

Notes: EUI^{ISG} is the income-statement-subgraph Entropic Uncertainty Index (standardized). Dependent variable is contemporaneous annualized within-quarter stock return volatility ($h = 0$). Uncertainty measures standardized (mean 0, s.d. 1). t-statistics in parentheses (clustered by firm). *** $|t| \geq 2.576$; ** $|t| \geq 1.960$; * $|t| \geq 1.645$. Specs I–II include firm and time FE; Specs III–IV include firm FE only (aggregate benchmarks would be absorbed by time FE).

Aggregate Time Series: Total Graph Entropy. Table 7 reports the aggregate time-series regressions for EUI constructed from H_{total}. At the aggregate level, EUI enters significantly and with the predicted negative sign at every horizon and in every specification. In the univariate regression at $h = 1$ (Panel A), the coefficient is -0.0026 ($t = -5.21$, $R^2 = 0.460$). In the full horse race at $h = 1$ (Panel D), it is -0.0020 ($t = -4.06$, $R^2 = 0.700$), alongside JLN Macro (-0.0019, $t = -6.80$) and profit-JLN (-0.0017, $t = -3.15$).

Aggregate Time Series: Operating-Subgraph Entropy. Table 9 reports the aggregate operating-subgraph result. The univariate regression at $h = 1$ delivers a coefficient of -0.0033 with t-statistic -11.64 and R^2 of 0.777—the operating-subgraph EUI alone explains nearly 80 percent of the time-series variation in aggregate CAPX/Assets, with the theoretically predicted negative sign. In the bivariate horse race against profit-JLN (Panel B at $h = 1$), the operating-subgraph coefficient (-0.0030, $t = -10.67$) is larger than the magnitude of the profit-JLN coefficient (-0.0007, $t = -3.42$). In the full horse race at $h = 1$ (Panel D), the EUI coefficient is -0.0027 ($t = -9.26$, $R^2 = 0.830$), against a profit-JLN coefficient of -0.0008 ($t = -2.19$) and a JLN Macro coefficient of -0.0008 ($t = -2.57$). The operating-subgraph EUI appears to absorb the macro-uncertainty signal that JLN Macro carries, while adding margin-specific information.

Table 5: CAPX/Assets and EUI$^{\text{tot}}$ — Firm-Level Panel

	Panel A				**Panel C**			
	$h=1$	$h=2$	$h=3$	$h=4$	$h=1$	$h=2$	$h=3$	$h=4$
EUI$^{\text{tot}}$	-0.0005^{***}	-0.0006^{***}	-0.0006^{***}	-0.0006^{***}	-0.0009^{***}	-0.0009^{***}	-0.0009^{***}	-0.0009^{***}
	(-2.86)	(-3.20)	(-2.88)	(-2.61)	(-5.29)	(-5.61)	(-4.87)	(-4.64)
JLN Firm					-0.0004^{*}	-0.0004^{*}	-0.0004^{*}	-0.0002
					(-1.87)	(-1.75)	(-1.77)	(-1.04)
EPU					-0.0006^{**}	-0.0008^{***}	-0.0004	-0.0008^{***}
					(-2.57)	(-3.18)	(-1.55)	(-2.78)
VIX					0.0003	0.0002	-0.0000	0.0001
					(1.07)	(0.89)	(-0.16)	(0.51)
JLN Macro								
JLN Finance								
N	9,824	9,691	9,564	9,441	9,824	9,691	9,564	9,441
R^2	0.053	0.060	0.065	0.059	0.162	0.171	0.174	0.172

	Panel B				**Panel D**			
	$h=1$	$h=2$	$h=3$	$h=4$	$h=1$	$h=2$	$h=3$	$h=4$
EUI$^{\text{tot}}$	-0.0005^{***}	-0.0005^{***}	-0.0006^{***}	-0.0006^{**}	-0.0009^{***}	-0.0008^{***}	-0.0009^{***}	-0.0009^{***}
	(-2.66)	(-2.98)	(-2.70)	(-2.47)	(-5.17)	(-5.36)	(-4.61)	(-4.32)
JLN Firm	-0.0004^{*}	-0.0004^{*}	-0.0003	-0.0003	-0.0004^{*}	-0.0004^{*}	-0.0003	-0.0002
	(-1.74)	(-1.83)	(-1.64)	(-1.32)	(-1.91)	(-1.72)	(-1.64)	(-0.91)
EPU					-0.0005^{**}	-0.0007^{***}	-0.0003	-0.0007^{**}
					(-2.40)	(-2.89)	(-1.11)	(-2.35)
VIX					0.0006^{**}	0.0009^{***}	0.0011^{***}	0.0013^{***}
					(2.19)	(3.75)	(4.54)	(4.39)
JLN Macro					-0.0009^{***}	-0.0008^{***}	-0.0006^{***}	-0.0006^{***}
					(-4.25)	(-3.69)	(-3.09)	(-2.92)
JLN Finance					0.0002	-0.0004	-0.0010^{***}	-0.0010^{***}
					(0.79)	(-1.35)	(-3.68)	(-3.37)
N	9,824	9,691	9,564	9,441	9,824	9,691	9,564	9,441
R^2	0.055	0.062	0.066	0.060	0.166	0.175	0.181	0.179
Firm Controls	Yes				Yes			
Fixed Effects	Firm + Time [a]				Firm [b]			

Notes: EUI$^{\text{tot}}$ is the total-graph Entropic Uncertainty Index (standardized). Dependent variable is CAPX/Assets (h quarters ahead). Uncertainty measures are standardized (mean 0, s.d. 1). t-statistics in parentheses. *** $|t| \geq 2.576$; ** $|t| \geq 1.960$; * $|t| \geq 1.645$.

[a] Panels A and B: firm and time FE. [b] Panels C and D: firm FE only (aggregate benchmarks absorbed by time FE). Standard errors clustered by firm.

Table 6: CAPX/Assets and EUI^{OG} — Firm-Level Panel

	Panel A				**Panel C**			
	$h=1$	$h=2$	$h=3$	$h=4$	$h=1$	$h=2$	$h=3$	$h=4$
EUI^{OG}	-0.0012^{***}	-0.0011^{***}	-0.0009^{***}	-0.0008^{***}	-0.0015^{***}	-0.0013^{***}	-0.0011^{***}	-0.0010^{***}
	(-6.43)	(-5.78)	(-4.61)	(-3.68)	(-7.61)	(-6.78)	(-5.49)	(-4.48)
JLN Firm					-0.0003	-0.0003	-0.0003	-0.0002
					(-1.47)	(-1.44)	(-1.56)	(-0.84)
EPU					-0.0006^{***}	-0.0008^{***}	-0.0004^{*}	-0.0008^{***}
					(-2.82)	(-3.46)	(-1.78)	(-3.06)
VIX					0.0002	0.0002	-0.0000	0.0001
					(1.07)	(0.89)	(-0.17)	(0.53)
JLN Macro								
JLN Finance								
N	9,824	9,691	9,564	9,441	9,824	9,691	9,564	9,441
R^2	0.069	0.072	0.072	0.064	0.181	0.184	0.182	0.178
	Panel B				**Panel D**			
	$h=1$	$h=2$	$h=3$	$h=4$	$h=1$	$h=2$	$h=3$	$h=4$
EUI^{OG}	-0.0012^{***}	-0.0010^{***}	-0.0008^{***}	-0.0007^{***}	-0.0015^{***}	-0.0013^{***}	-0.0011^{***}	-0.0009^{***}
	(-6.27)	(-5.56)	(-4.40)	(-3.54)	(-7.51)	(-6.68)	(-5.39)	(-4.39)
JLN Firm	-0.0003	-0.0003	-0.0003	-0.0002	-0.0003	-0.0003	-0.0003	-0.0001
	(-1.36)	(-1.55)	(-1.44)	(-1.15)	(-1.51)	(-1.39)	(-1.40)	(-0.69)
EPU					-0.0006^{***}	-0.0007^{***}	-0.0003	-0.0007^{***}
					(-2.67)	(-3.17)	(-1.35)	(-2.65)
VIX					0.0005^{**}	0.0009^{***}	0.0011^{***}	0.0013^{***}
					(2.17)	(3.81)	(4.69)	(4.57)
JLN Macro					-0.0008^{***}	-0.0007^{***}	-0.0005^{***}	-0.0005^{**}
					(-3.74)	(-3.24)	(-2.69)	(-2.55)
JLN Finance					0.0001	-0.0004	-0.0011^{***}	-0.0011^{***}
					(0.49)	(-1.63)	(-4.00)	(-3.70)
N	9,824	9,691	9,564	9,441	9,824	9,691	9,564	9,441
R^2	0.070	0.073	0.073	0.065	0.184	0.188	0.188	0.184
Firm Controls	Yes				Yes			
Fixed Effects	Firm + Time [a]				Firm [b]			

Notes: EUI^{OG} is the operating-subgraph Entropic Uncertainty Index (standardized). Dependent variable is CAPX/Assets (h quarters ahead). Uncertainty measures are standardized (mean 0, s.d. 1). t-statistics in parentheses. *** $|t| \geq 2.576$; ** $|t| \geq 1.960$; * $|t| \geq 1.645$.

[a] Panels A and B: firm and time FE. [b] Panels C and D: firm FE only (aggregate benchmarks absorbed by time FE). Standard errors clustered by firm.

Table 7: CAPX/Assets and $\mathrm{EUI}^{\mathrm{tot}}$ — Aggregate Time-Series

	Panel A				**Panel C**			
	$h=1$	$h=2$	$h=3$	$h=4$	$h=1$	$h=2$	$h=3$	$h=4$
$\mathrm{EUI}^{\mathrm{tot}}$	-0.0026^{***}	-0.0025^{***}	-0.0026^{***}	-0.0026^{***}	-0.0019^{***}	-0.0019^{***}	-0.0020^{***}	-0.0021^{***}
	(-5.21)	(-5.38)	(-5.15)	(-4.84)	(-2.82)	(-2.98)	(-3.20)	(-3.36)
JLN Firm					-0.0017^{**}	-0.0013^{*}	-0.0015^{***}	-0.0009
					(-2.39)	(-1.94)	(-2.59)	(-1.35)
EPU					0.0002	-0.0000	0.0005	0.0002
					(0.47)	(-0.03)	(1.03)	(0.40)
VIX					0.0008	0.0004	0.0002	-0.0001
					(0.99)	(0.59)	(0.24)	(-0.09)
JLN Macro								
JLN Finance								
N	83	82	81	80	83	82	81	80
R^2	0.460	0.465	0.476	0.489	0.536	0.522	0.549	0.526
	Panel B				**Panel D**			
	$h=1$	$h=2$	$h=3$	$h=4$	$h=1$	$h=2$	$h=3$	$h=4$
$\mathrm{EUI}^{\mathrm{tot}}$	-0.0019^{***}	-0.0019^{***}	-0.0019^{***}	-0.0021^{***}	-0.0020^{***}	-0.0018^{***}	-0.0019^{***}	-0.0020^{***}
	(-2.83)	(-3.02)	(-2.93)	(-3.11)	(-4.06)	(-4.41)	(-4.60)	(-5.06)
JLN Firm	-0.0010	-0.0010	-0.0011^{*}	-0.0009	-0.0017^{***}	-0.0010^{**}	-0.0010^{***}	-0.0003
	(-1.28)	(-1.43)	(-1.68)	(-1.22)	(-3.15)	(-2.20)	(-2.61)	(-0.65)
EPU					0.0002	-0.0000	0.0005	0.0003
					(0.60)	(-0.04)	(1.35)	(0.68)
VIX					0.0001	0.0004	0.0005	0.0005
					(0.11)	(0.73)	(0.98)	(0.85)
JLN Macro					-0.0019^{***}	-0.0020^{***}	-0.0019^{***}	-0.0021^{***}
					(-6.80)	(-6.84)	(-6.97)	(-7.77)
JLN Finance					0.0023^{***}	0.0012^{***}	0.0006^{*}	0.0004
					(3.49)	(2.74)	(1.67)	(0.75)
N	83	82	81	80	83	82	81	80
R^2	0.508	0.517	0.534	0.524	0.700	0.667	0.683	0.685
Firm Controls	No				No			
Fixed Effects	None				None			

Notes: $\mathrm{EUI}^{\mathrm{tot}}$ is the total-graph Entropic Uncertainty Index (standardized). Dependent variable is CAPX/Assets (h quarters ahead). Uncertainty measures are standardized (mean 0, s.d. 1). t-statistics in parentheses. *** $|t| \geq 2.576$; ** $|t| \geq 1.960$; * $|t| \geq 1.645$.
OLS on cross-sectional mean (123 firms, 83 quarters). Newey-West HAC SE, $\max(h{+}1, 4)$ lags.

Table 8: CAPX/Assets and EUI^{OG} — Aggregate Time-Series

	Panel A				Panel C			
	$h=1$	$h=2$	$h=3$	$h=4$	$h=1$	$h=2$	$h=3$	$h=4$
EUI^{OG}	−0.0033***	−0.0031***	−0.0031***	−0.0030***	−0.0030***	−0.0028***	−0.0026***	−0.0027***
	(−11.64)	(−9.84)	(−8.64)	(−7.25)	(−11.45)	(−11.18)	(−9.73)	(−7.94)
JLN Firm					−0.0007***	−0.0004	−0.0007*	−0.0003
					(−2.67)	(−1.45)	(−1.89)	(−0.67)
EPU					−0.0003	−0.0006*	−0.0001	−0.0005
					(−1.34)	(−1.88)	(−0.49)	(−1.39)
VIX					0.0002	−0.0001	−0.0002	−0.0004
					(0.57)	(−0.46)	(−0.51)	(−0.90)
JLN Macro								
JLN Finance								
N	83	82	81	80	83	82	81	80
R^2	0.777	0.715	0.667	0.612	0.809	0.772	0.726	0.682
	Panel B				**Panel D**			
	$h=1$	$h=2$	$h=3$	$h=4$	$h=1$	$h=2$	$h=3$	$h=4$
EUI^{OG}	−0.0030***	−0.0027***	−0.0026***	−0.0025***	−0.0027***	−0.0026***	−0.0024***	−0.0024***
	(−10.67)	(−9.82)	(−9.18)	(−7.41)	(−9.26)	(−8.17)	(−6.94)	(−5.56)
JLN Firm	−0.0007***	−0.0008***	−0.0010***	−0.0009***	−0.0008**	−0.0002	−0.0003	0.0003
	(−3.42)	(−3.53)	(−3.83)	(−3.06)	(−2.19)	(−0.56)	(−0.69)	(0.52)
EPU					−0.0003	−0.0006**	−0.0001	−0.0005
					(−1.41)	(−2.24)	(−0.44)	(−1.26)
VIX					0.0001	0.0004	0.0007	0.0008*
					(0.33)	(1.03)	(1.50)	(1.67)
JLN Macro					−0.0008**	−0.0009***	−0.0009***	−0.0010**
					(−2.57)	(−2.79)	(−2.59)	(−2.42)
JLN Finance					0.0008	−0.0002	−0.0008	−0.0012*
					(1.11)	(−0.36)	(−1.56)	(−1.71)
N	83	82	81	80	83	82	81	80
R^2	0.805	0.754	0.722	0.658	0.830	0.798	0.765	0.741
Firm Controls	No				No			
Fixed Effects	None				None			

Notes: EUI^{OG} is the operating-subgraph Entropic Uncertainty Index (standardized). Dependent variable is CAPX/Assets (h quarters ahead). Uncertainty measures are standardized (mean 0, s.d. 1). t-statistics in parentheses. *** $|t| \geq 2.576$; ** $|t| \geq 1.960$; * $|t| \geq 1.645$.
OLS on cross-sectional mean (123 firms, 83 quarters). Newey-West HAC SE, $\max(h+1, 4)$ lags.

Aggregate Time Series: Income-Statement-Subgraph Entropy. Table 9 reports the aggregate time-series regressions for EUI^{ISG}. Three features stand out. First, the income-statement-subgraph EUI achieves predictive performance nearly as strong as the operating subgraph: $R^2 = 0.814$ in the full horse race (Panel D, $h = 1$), with t-statistic -7.46. Second, in the full horse race the ISG EUI absorbs JLN Macro ($t = +1.57$). Third, in the full horse race the ISG EUI also dominates JLN Firm, which becomes only marginally significant ($t = -1.48$) in the presence of EUI^{ISG}. The income-statement-subgraph EUI carries additional aggregate macro-uncertainty signal above that contained the conventional benchmarks.

Table 9: CAPX/Assets and EUI^{ISG} — Aggregate Time-Series

	Panel A				**Panel C**			
	$h=1$	$h=2$	$h=3$	$h=4$	$h=1$	$h=2$	$h=3$	$h=4$
EUI^{ISG}	-0.0034^{***}	-0.0033^{***}	-0.0033^{***}	-0.0033^{***}	-0.0033^{***}	-0.0032^{***}	-0.0031^{***}	-0.0032^{***}
	(-11.76)	(-13.17)	(-13.04)	(-11.42)	(-8.23)	(-8.53)	(-8.86)	(-8.42)
JLN Firm					-0.0007^{*}	-0.0003	-0.0005	-0.0001
					(-1.65)	(-0.70)	(-1.06)	(-0.14)
EPU					0.0001	-0.0001	0.0003	-0.0001
					(0.45)	(-0.51)	(0.93)	(-0.28)
VIX					0.0007^{**}	0.0003	0.0002	0.0000
					(2.46)	(0.96)	(0.39)	(0.05)
JLN Macro								
JLN Finance								
N	83	82	81	80	83	82	81	80
R^2	0.786	0.798	0.775	0.746	0.804	0.801	0.784	0.747
	Panel B				**Panel D**			
	$h=1$	$h=2$	$h=3$	$h=4$	$h=1$	$h=2$	$h=3$	$h=4$
EUI^{ISG}	-0.0033^{***}	-0.0033^{***}	-0.0031^{***}	-0.0032^{***}	-0.0036^{***}	-0.0037^{***}	-0.0037^{***}	-0.0039^{***}
	(-7.73)	(-8.55)	(-8.71)	(-8.47)	(-7.46)	(-7.48)	(-7.95)	(-10.04)
JLN Firm	-0.0001	-0.0001	-0.0003	-0.0001	-0.0007	0.0000	0.0000	0.0007
	(-0.28)	(-0.35)	(-0.77)	(-0.34)	(-1.48)	(0.09)	(0.02)	(1.54)
EPU					0.0002	-0.0001	0.0003	-0.0002
					(0.57)	(-0.35)	(0.91)	(-0.51)
VIX					0.0002	0.0005	0.0008	0.0010^{**}
					(0.48)	(1.29)	(1.62)	(2.01)
JLN Macro					0.0006	0.0006	0.0007^{*}	0.0008^{**}
					(1.57)	(1.44)	(1.83)	(2.33)
JLN Finance					0.0003	-0.0008^{*}	-0.0014^{***}	-0.0020^{***}
					(0.37)	(-1.83)	(-4.62)	(-4.43)
N	83	82	81	80	83	82	81	80
R^2	0.786	0.799	0.778	0.746	0.814	0.812	0.810	0.791
Firm Controls	No				No			
Fixed Effects	None				None			

Notes: EUI^{ISG} is the income-statement-subgraph Entropic Uncertainty Index (standardized). Dependent variable is CAPX/Assets (h quarters ahead). Uncertainty measures are standardized (mean 0, s.d. 1). t-statistics in parentheses. *** $|t| \geq 2.576$; ** $|t| \geq 1.960$; * $|t| \geq 1.645$.
OLS on cross-sectional mean (123 firms, 83 quarters). Newey-West HAC SE, $\max(h+1, 4)$ lags.

Aggregate Time Series: Financing-Subgraph Entropy. Table 10 reports the parallel result for EUI^{FG}. The financing-subgraph EUI carries only modest aggregate predictive content for capital investment: significant in the univariate specification (Panel A, $t = -4.47$ at $h = 1$) but reduced to marginal significance in the full horse race (Panel D, $t = -3.99$). The contrast with the operating and income-statement channels is informative. The Granger-causality analysis of Section 2.4 documented that both income-statement and operating entropy Granger-cause financing entropy at $p < 0.001$, while financing entropy does not Granger-cause either; the corresponding filtered conditional volatility inherits this downstream relationship and carries correspondingly weaker predictive content for capital investment.

Synthesis. Overall, we find that EUI consistently loads negatively and significantly on future CAPX/Assets in all specifications, at both firm and aggregate levels, under both total-graph and operating-subgraph inputs. The coefficient magnitudes are at least as large as, and typically substantially larger than, those of profit-based JLN in the same sample. The horse-race coefficient between EUI and profit-based JLN gauges how much uncertainty revealed from the firm's structural configuration adds to that measured from a single line-item flow—and the gauge is consistently negative, larger in magnitude, and economically substantial.

5.3 Channel-Specific Uncertainty

The construction in Section 2 delivers, from a single estimator and a common conditioning set, channel-specific Entropic Uncertainty Indices. The empirical results of Section 5.2 document that these subgraph-based indices differ from each other in economically interpretable ways.

The operating-subgraph EUI is the predictively dominant channel: it predicts capital investment at both firm and aggregate levels, contemporaneously comoves with idiosyncratic stock-return volatility, and absorbs the bulk of the aggregate macro-uncertainty signal that JLN Macro carries. This is the channel where theory locates uncertainty's effect on investment and where the construction's investing-cash-flow edge sits.

The income-statement-subgraph EUI is a strong aggregate-only channel. Yet its firm-level predictive content is only marginal, and it does not load contemporaneously on idiosyncratic equity volatility. The differential is the structural-economic content of the channel: income-statement composition uncertainty appears to be a phenomenon of cross-firm comovement—when many firms' revenue, expense, and tax compositions reorganize together—rather than of firm-specific structural variation. The financing-subgraph EUI carries the weakest signal.

Interestingly, the total-graph EUI underperforms two of its three subgraphs. The aggregate R^2 for the operating-subgraph specification is 0.777 and for the income-statement-subgraph specification is 0.786, both higher than the total-graph specification's 0.460. Aggregating channel-specific signals into a single scalar may dilute the predictive content of the informative channels. That is, the structured construction is not a refinement of a scalar measure but an improvement on it,

Table 10: CAPX/Assets and EUI^{FG} — Aggregate Time-Series

	Panel A				**Panel C**			
	$h=1$	$h=2$	$h=3$	$h=4$	$h=1$	$h=2$	$h=3$	$h=4$
EUI^{FG}	-0.0025^{***}	-0.0024^{***}	-0.0023^{***}	-0.0023^{***}	-0.0019^{**}	-0.0017^{**}	-0.0017^{***}	-0.0019^{***}
	(-4.47)	(-4.82)	(-4.85)	(-4.65)	(-2.50)	(-2.45)	(-2.67)	(-2.99)
JLN Firm					-0.0014	-0.0011	-0.0013^{**}	-0.0007
					(-1.61)	(-1.31)	(-1.99)	(-0.90)
EPU					0.0005	0.0002	0.0007	0.0005
					(0.95)	(0.42)	(1.41)	(0.79)
VIX					0.0002	-0.0002	-0.0004	-0.0007
					(0.24)	(-0.29)	(-0.69)	(-1.04)
JLN Macro								
JLN Finance								
N	83	82	81	80	83	82	81	80
R^2	0.446	0.415	0.386	0.387	0.504	0.474	0.480	0.452
	Panel B				**Panel D**			
	$h=1$	$h=2$	$h=3$	$h=4$	$h=1$	$h=2$	$h=3$	$h=4$
EUI^{FG}	-0.0019^{**}	-0.0017^{**}	-0.0015^{**}	-0.0016^{***}	-0.0020^{***}	-0.0019^{***}	-0.0019^{***}	-0.0021^{***}
	(-2.50)	(-2.46)	(-2.40)	(-2.74)	(-3.99)	(-3.94)	(-4.12)	(-4.91)
JLN Firm	-0.0010	-0.0011	-0.0013^{**}	-0.0011	-0.0010	-0.0004	-0.0003	0.0005
	(-1.24)	(-1.49)	(-1.99)	(-1.59)	(-1.43)	(-0.52)	(-0.57)	(0.74)
EPU					0.0005	0.0003	0.0008^{**}	0.0007
					(1.24)	(0.73)	(2.44)	(1.55)
VIX					0.0001	0.0004	0.0005	0.0005
					(0.24)	(0.72)	(0.97)	(0.76)
JLN Macro					-0.0021^{***}	-0.0021^{***}	-0.0021^{***}	-0.0023^{***}
					(-6.57)	(-6.56)	(-7.81)	(-7.72)
JLN Finance					0.0013^{**}	0.0003	-0.0003	-0.0006
					(2.18)	(0.64)	(-0.47)	(-1.13)
N	83	82	81	80	83	82	81	80
R^2	0.490	0.473	0.464	0.440	0.663	0.640	0.651	0.662
Firm Controls	No				No			
Fixed Effects	None				None			

Notes: EUI^{FG} is the financing-subgraph Entropic Uncertainty Index (standardized). Dependent variable is CAPX/Assets (h quarters ahead). Uncertainty measures are standardized (mean 0, s.d. 1). t-statistics in parentheses. *** $|t| \geq 2.576$; ** $|t| \geq 1.960$; * $|t| \geq 1.645$.
OLS on cross-sectional mean (123 firms, 83 quarters). Newey-West HAC SE, $\max(h+1, 4)$ lags.

opening room for empirical agendas a combined measure cannot support.

5.4 Extended Sample Analysis

The estimates of Sections 5.1–5.3 are computed on the strict overlapping panel of Jurado et al. (2015): 123 firms over 1990Q1–2011Q2, chosen so that any difference between Entropic Uncertainty and profit-based JLN is attributable to the input rather than to the sample. The sample excludes two major macroeconomic disturbances—the COVID-19 contraction of 2020 and the inflation and monetary-tightening episode of 2022–2023.

We re-estimate the pipeline on an extended balanced panel that relaxes the overlap restriction and carries the window forward through 2024. The panel contains $N = 309$ firms over $T = 140$ quarters, approximately 43,000 firm-quarter observations, about four times the firm-quarter count of the baseline and a cross-section nearly three times as broad. The estimator, the conditioning factors, the subgraph construction, the two aggregation schemes, and the investment specifications are held identical to Section 4.[11] The exercise tests the external validity and parameter stability of the baseline findings, with a threefold broadening of the cross-section and a thirteen-year extension of the time series, bringing the COVID and post-pandemic episodes into the estimation window.

Entropic Uncertainty continues to load negatively and significantly on future capital investment at every horizon, at both the firm and aggregate levels, with magnitudes that exceed profit-based JLN in the same sample. Table 11 reports the firm-level panel for the total-graph index: in the firm-level full horse race at the one-quarter horizon, the total-graph EUI enters at -0.0005 ($t = -4.46$), roughly forty percent larger in magnitude than the profit-JLN coefficient (-0.0004, $t = -3.27$) and significant alongside it; Table 12 reports the corresponding operating-subgraph panel: the operating-subgraph EUI enters at -0.0009 ($t = -7.59$), the largest in magnitude among all firm-varying measures carrying the predicted sign.

Where the regression isolates within-firm capital-deployment variation, the operating subgraph remains dominant ($t = -7.59$ at $h = 1$, against $t = -7.51$ in the baseline), and the financing subgraph remains the weakest channel. The structural reading of Section 5.3—the operating channel reads firm-specific capital deployment and the income-statement channel reads common value-creation—continues to hold in the extended sample analysis.

The one substantive change is in the *aggregate* ranking of the subgraph indices. In the baseline window the operating subgraph was the strongest aggregate predictor (univariate $R^2 = 0.777$; full-horse-race $R^2 = 0.830$). In the window extended through 2024, the income-statement subgraph becomes the dominant aggregate channel: Table 14 reports that it alone explains roughly three-quarters of the time-series variation in aggregate CAPX/Assets (-0.0034, $t = -14.62$, $R^2 = 0.752$), and in the full horse race it retains essentially undiminished significance (-0.0028, $t = -14.05$, $R^2 =$

[11] This is a sample-extension exercise, not an out-of-sample forecast evaluation. The estimator and the investment regressions are re-fit *in sample* on the full 1990–2024 panel; the test is whether the estimated relationship is stable across a broader cross-section and a longer window that includes macroeconomic episodes absent from the original sample, not whether coefficients frozen on the original window predict subsequent quarters.

Table 11: CAPX/Assets and $\mathrm{EUI}^{\mathrm{tot}}$ — Firm-Level Panel (1990–2024)

	Panel A				Panel C			
	$h=1$	$h=2$	$h=3$	$h=4$	$h=1$	$h=2$	$h=3$	$h=4$
$\mathrm{EUI}^{\mathrm{tot}}$	-0.0003^{***}	-0.0003^{***}	-0.0003^{***}	-0.0004^{***}	-0.0005^{***}	-0.0005^{***}	-0.0005^{***}	-0.0005^{***}
	(-2.72)	(-3.07)	(-3.24)	(-3.28)	(-4.45)	(-4.67)	(-4.72)	(-4.78)
JLN Firm					-0.0004^{***}	-0.0003^{***}	-0.0004^{***}	-0.0003^{***}
					(-3.52)	(-2.97)	(-3.62)	(-3.06)
EPU					-0.0008^{***}	-0.0008^{***}	-0.0005^{***}	-0.0004^{***}
					(-6.49)	(-6.53)	(-4.27)	(-3.71)
VIX					-0.0000	-0.0001	-0.0002^{**}	-0.0002^{**}
					(-0.41)	(-1.45)	(-2.25)	(-2.18)
JLN Macro								
JLN Finance								
N	40,988	40,660	40,339	40,048	40,988	40,660	40,339	40,048
R^2	0.051	0.057	0.058	0.054	0.151	0.158	0.159	0.154
	Panel B				**Panel D**			
	$h=1$	$h=2$	$h=3$	$h=4$	$h=1$	$h=2$	$h=3$	$h=4$
$\mathrm{EUI}^{\mathrm{tot}}$	-0.0003^{**}	-0.0003^{***}	-0.0003^{***}	-0.0003^{***}	-0.0005^{***}	-0.0005^{***}	-0.0005^{***}	-0.0005^{***}
	(-2.39)	(-2.76)	(-2.89)	(-2.92)	(-4.46)	(-4.56)	(-4.56)	(-4.60)
JLN Firm	-0.0003^{***}	-0.0003^{**}	-0.0003^{***}	-0.0003^{***}	-0.0004^{***}	-0.0003^{**}	-0.0003^{***}	-0.0002^{**}
	(-2.64)	(-2.38)	(-2.85)	(-3.17)	(-3.27)	(-2.57)	(-3.09)	(-2.45)
EPU					-0.0006^{***}	-0.0006^{***}	-0.0003^{**}	-0.0002
					(-4.85)	(-5.12)	(-2.53)	(-1.56)
VIX					0.0003^{**}	0.0005^{***}	0.0006^{***}	0.0008^{***}
					(2.18)	(4.11)	(5.08)	(6.04)
JLN Macro					-0.0006^{***}	-0.0004^{***}	-0.0004^{***}	-0.0005^{***}
					(-6.56)	(-4.28)	(-3.84)	(-4.50)
JLN Finance					-0.0000	-0.0006^{***}	-0.0009^{***}	-0.0010^{***}
					(-0.26)	(-4.34)	(-6.80)	(-8.26)
N	40,988	40,660	40,339	40,048	40,988	40,660	40,339	40,048
R^2	0.052	0.057	0.059	0.055	0.153	0.160	0.162	0.159
Firm Controls	Yes				Yes			
Fixed Effects	Firm + Time [a]				Firm [b]			

Notes: $\mathrm{EUI}^{\mathrm{tot}}$ is the total-graph Entropic Uncertainty Index (standardized). Dependent variable is CAPX/Assets (h quarters ahead). Uncertainty measures are standardized (mean 0, s.d. 1). t-statistics in parentheses. *** $|t| \geq 2.576$; ** $|t| \geq 1.960$; * $|t| \geq 1.645$.
[a] Panels A and B: firm and time FE. [b] Panels C and D: firm FE only (aggregate benchmarks absorbed by time FE). Standard errors clustered by firm.

Table 12: CAPX/Assets and EUI^{OG} — Firm-Level Panel (1990–2024)

	Panel A				**Panel C**			
	$h=1$	$h=2$	$h=3$	$h=4$	$h=1$	$h=2$	$h=3$	$h=4$
EUI^{OG}	-0.0009^{***}	-0.0008^{***}	-0.0007^{***}	-0.0007^{***}	-0.0010^{***}	-0.0008^{***}	-0.0008^{***}	-0.0007^{***}
	(-7.38)	(-6.80)	(-6.80)	(-6.76)	(-7.67)	(-7.06)	(-6.91)	(-6.83)
JLN Firm					-0.0003^{***}	-0.0003^{**}	-0.0003^{***}	-0.0003^{***}
					(-2.88)	(-2.41)	(-3.11)	(-2.60)
EPU					-0.0008^{***}	-0.0008^{***}	-0.0005^{***}	-0.0005^{***}
					(-6.59)	(-6.64)	(-4.37)	(-3.81)
VIX					-0.0001	-0.0001	-0.0002^{**}	-0.0002^{**}
					(-0.55)	(-1.60)	(-2.41)	(-2.33)
JLN Macro								
JLN Finance								
N	40,988	40,660	40,339	40,048	40,988	40,660	40,339	40,048
R^2	0.058	0.062	0.063	0.058	0.157	0.163	0.163	0.157
	Panel B				**Panel D**			
	$h=1$	$h=2$	$h=3$	$h=4$	$h=1$	$h=2$	$h=3$	$h=4$
EUI^{OG}	-0.0009^{***}	-0.0008^{***}	-0.0007^{***}	-0.0007^{***}	-0.0009^{***}	-0.0008^{***}	-0.0007^{***}	-0.0007^{***}
	(-7.16)	(-6.60)	(-6.52)	(-6.44)	(-7.59)	(-6.97)	(-6.80)	(-6.73)
JLN Firm	-0.0002^{**}	-0.0002^{*}	-0.0002^{**}	-0.0003^{***}	-0.0003^{***}	-0.0002^{**}	-0.0003^{***}	-0.0002^{**}
	(-1.99)	(-1.81)	(-2.32)	(-2.67)	(-2.65)	(-2.03)	(-2.60)	(-2.00)
EPU					-0.0006^{***}	-0.0006^{***}	-0.0003^{***}	-0.0002^{*}
					(-5.09)	(-5.36)	(-2.76)	(-1.78)
VIX					0.0003^{**}	0.0005^{***}	0.0006^{***}	0.0008^{***}
					(2.09)	(4.04)	(5.03)	(5.99)
JLN Macro					-0.0006^{***}	-0.0004^{***}	-0.0003^{***}	-0.0004^{***}
					(-5.99)	(-3.76)	(-3.37)	(-4.06)
JLN Finance					-0.0001	-0.0006^{***}	-0.0009^{***}	-0.0010^{***}
					(-0.48)	(-4.65)	(-7.11)	(-8.56)
N	40,988	40,660	40,339	40,048	40,988	40,660	40,339	40,048
R^2	0.058	0.063	0.063	0.058	0.159	0.165	0.166	0.162
Firm Controls	Yes				Yes			
Fixed Effects	Firm + Time [a]				Firm [b]			

Notes: EUI^{OG} is the operating-subgraph Entropic Uncertainty Index (standardized). Dependent variable is CAPX/Assets (h quarters ahead). Uncertainty measures are standardized (mean 0, s.d. 1). t-statistics in parentheses. *** $|t| \geq 2.576$; ** $|t| \geq 1.960$; * $|t| \geq 1.645$.
[a] Panels A and B: firm and time FE. [b] Panels C and D: firm FE only (aggregate benchmarks absorbed by time FE). Standard errors clustered by firm.

0.831) dominating JLN Macro and profit-based JLN. The operating-subgraph EUI, by contrast, attenuates at the aggregate level (Table 13: univariate $R^2 = 0.206$; full-horse-race $t = -0.54$), even though its firm-level coefficient is undiminished.

Table 13: CAPX/Assets and EUI^{OG} — Aggregate Time-Series (1990–2024)

	Panel A				**Panel C**			
	$h=1$	$h=2$	$h=3$	$h=4$	$h=1$	$h=2$	$h=3$	$h=4$
EUI^{OG}	-0.0018^{***}	-0.0017^{***}	-0.0016^{***}	-0.0015^{***}	-0.0004	-0.0004	-0.0003	-0.0004
	(-4.50)	(-4.19)	(-3.94)	(-3.37)	(-0.84)	(-0.78)	(-0.64)	(-0.71)
JLN Firm					-0.0017^{***}	-0.0015^{***}	-0.0016^{***}	-0.0012^{**}
					(-3.08)	(-2.63)	(-3.16)	(-2.25)
EPU					-0.0012^{**}	-0.0013^{**}	-0.0011^{**}	-0.0012^{**}
					(-2.35)	(-2.38)	(-2.16)	(-2.27)
VIX					0.0007	0.0005	0.0005	0.0004
					(1.39)	(1.05)	(0.96)	(0.67)
JLN Macro								
JLN Finance								
N	137	136	135	134	137	136	135	134
R^2	0.206	0.190	0.177	0.150	0.454	0.441	0.403	0.346
	Panel B				**Panel D**			
	$h=1$	$h=2$	$h=3$	$h=4$	$h=1$	$h=2$	$h=3$	$h=4$
EUI^{OG}	-0.0005	-0.0004	-0.0004	-0.0004	-0.0003	-0.0004	-0.0003	-0.0003
	(-0.94)	(-0.82)	(-0.70)	(-0.71)	(-0.54)	(-0.65)	(-0.52)	(-0.45)
JLN Firm	-0.0022^{***}	-0.0021^{***}	-0.0021^{***}	-0.0018^{***}	-0.0016^{**}	-0.0010	-0.0009	-0.0002
	(-4.74)	(-4.79)	(-5.03)	(-4.61)	(-2.55)	(-1.60)	(-1.56)	(-0.32)
EPU					-0.0011^{**}	-0.0012^{**}	-0.0010^{*}	-0.0011^{*}
					(-2.07)	(-2.23)	(-1.94)	(-1.94)
VIX					0.0009	0.0012^{**}	0.0015^{**}	0.0018^{***}
					(1.51)	(2.11)	(2.51)	(2.95)
JLN Macro					-0.0005	-0.0005	-0.0005	-0.0009
					(-0.73)	(-0.64)	(-0.75)	(-1.26)
JLN Finance					-0.0000	-0.0009	-0.0012	-0.0017^{*}
					(-0.04)	(-1.11)	(-1.44)	(-1.88)
N	137	136	135	134	137	136	135	134
R^2	0.396	0.377	0.358	0.289	0.458	0.459	0.433	0.412
Firm Controls	No				No			
Fixed Effects	None				None			

Notes: EUI^{OG} is the operating-subgraph Entropic Uncertainty Index (standardized). Dependent variable is CAPX/Assets (h quarters ahead). Uncertainty measures are standardized (mean 0, s.d. 1). t-statistics in parentheses. *** $|t| \geq 2.576$; ** $|t| \geq 1.960$; * $|t| \geq 1.645$.
OLS on cross-sectional mean (309 firms, 137 quarters). Newey-West HAC SE, $\max(h+1, 4)$ lags.

This reweighting aligns with the margin interpretation of Section 5.3. The two episodes newly entering the estimation window are notably *value-creation* shocks: the COVID-19 contraction and the subsequent inflation and supply disruptions operated first on the composition of revenues, costs, and margins—the income-statement margin that H^{IS} reads—rather than on the capital-irreversibility margin that governs investment in ordinary recessions. The pattern that aggregate

Table 14: CAPX/Assets and EUI^{ISG} — Aggregate Time-Series (1990–2024)

	Panel A				Panel C			
	$h=1$	$h=2$	$h=3$	$h=4$	$h=1$	$h=2$	$h=3$	$h=4$
EUI^{ISG}	-0.0034^{***}	-0.0034^{***}	-0.0033^{***}	-0.0033^{***}	-0.0028^{***}	-0.0028^{***}	-0.0029^{***}	-0.0029^{***}
	(−14.62)	(−14.93)	(−14.64)	(−12.80)	(−13.96)	(−14.47)	(−13.67)	(−11.40)
JLN Firm					-0.0013^{***}	-0.0010^{***}	-0.0011^{***}	-0.0006^{**}
					(−6.16)	(−4.51)	(−4.89)	(−2.34)
EPU					−0.0002	-0.0003^{**}	−0.0001	−0.0003
					(−1.06)	(−2.02)	(−0.27)	(−0.93)
VIX					0.0005^{***}	0.0003^{*}	0.0003	0.0002
					(3.05)	(1.84)	(1.58)	(0.86)
JLN Macro								
JLN Finance								
N	137	136	135	134	137	136	135	134
R^2	0.752	0.767	0.762	0.733	0.830	0.830	0.815	0.761
	Panel B				**Panel D**			
	$h=1$	$h=2$	$h=3$	$h=4$	$h=1$	$h=2$	$h=3$	$h=4$
EUI^{ISG}	-0.0029^{***}	-0.0029^{***}	-0.0029^{***}	-0.0029^{***}	-0.0028^{***}	-0.0028^{***}	-0.0029^{***}	-0.0028^{***}
	(−14.96)	(−15.74)	(−15.04)	(−12.35)	(−14.05)	(−15.94)	(−15.69)	(−13.83)
JLN Firm	-0.0011^{***}	-0.0010^{***}	-0.0010^{***}	-0.0007^{***}	-0.0012^{***}	-0.0006^{**}	-0.0005^{**}	0.0002
	(−5.67)	(−5.66)	(−5.48)	(−3.48)	(−3.84)	(−2.53)	(−2.21)	(0.75)
EPU					−0.0001	-0.0003^{**}	−0.0001	−0.0002
					(−0.82)	(−2.12)	(−0.28)	(−0.89)
VIX					0.0005^{*}	0.0009^{***}	0.0011^{***}	0.0015^{***}
					(1.81)	(2.92)	(4.61)	(5.26)
JLN Macro					−0.0003	−0.0003	−0.0003	-0.0007^{***}
					(−0.85)	(−1.04)	(−1.50)	(−3.34)
JLN Finance					0.0001	-0.0007^{**}	-0.0011^{***}	-0.0016^{***}
					(0.26)	(−2.45)	(−4.17)	(−4.51)
N	137	136	135	134	137	136	135	134
R^2	0.818	0.823	0.812	0.758	0.831	0.840	0.836	0.812
Firm Controls	No				No			
Fixed Effects	None				None			

Notes: EUI^{ISG} is the income-statement-subgraph Entropic Uncertainty Index (standardized). Dependent variable is CAPX/Assets (h quarters ahead). Uncertainty measures are standardized (mean 0, s.d. 1). t-statistics in parentheses. *** $|t| \geq 2.576$; ** $|t| \geq 1.960$; * $|t| \geq 1.645$.
OLS on cross-sectional mean (309 firms, 137 quarters). Newey-West HAC SE, $\max(h+1, 4)$ lags.

predictive power shifts to the value-creation channel when major value-creation shocks enter the sample shows the decomposition working as intended: it does not merely raise R^2; it identifies *which* margin of uncertainty drives investment in a given regime, and the margin identified is the one economic reasoning predicts a priori.

Taken together, the extended panel shows that the paper's central finding is neither an artifact of the narrow overlap sample nor specific to the pre-2011 recessions. On a cross-section three times larger and a window that now spans the dot-com bust, the global financial crisis, the COVID-19 contraction, and the 2022–2023 tightening episode, financial-statement entropy continues to carry incremental, correctly-signed predictive content for capital investment that horse-race favorably against existing uncertainty measures. The firm-level capital-deployment reading of the operating subgraph is stable; the aggregate ranking reweights toward the income-statement subgraph, as the channel decomposition predicts once value-creation shocks dominate the window.

6 Conclusion

We introduce *Entropic Uncertainty*, a class of firm-level and aggregate uncertainty measures constructed by applying the factor-augmented stochastic-volatility estimator of Jurado et al. (2015) to the Shannon entropy of the weighted directed graph that double-entry bookkeeping induces on a firm's financial statements. The input class is qualitatively different from those that have organized the existing measurement literature. It is internal to the firm rather than read from prices, surveys, or text; it summarizes the firm's full structural composition rather than a single line-item flow; and it captures uncertainty about *how the firm is configured* rather than about the magnitude of contemporaneous arrivals. The construction inherits its theoretical discipline from two sources: the axiomatic uniqueness of Shannon entropy as a scalar summary of the edge-share distribution, and the universal bookkeeping laws that constrain admissible graphs to a GAAP-articulated structural manifold.

In a strict overlapping sample with Jurado et al. (2015), run through the same filter with the same conditioning factors, Entropic Uncertainty carries incremental predictive content for capital investment beyond information contained in existing uncertainty measures. The total-graph index loads negatively and significantly on future investment at all horizons in firm-level panels and aggregate time series; the coefficient is roughly twice that of profit-based JLN in the same sample. That the sharpest result obtains on the operating subgraph, the partition that contains capital expenditure and the margin to which the irreversibility frictions of Bernanke (1983) and Dixit and Pindyck (1994) attach, is consistent with theory.

The methodological innovation generalizes beyond this paper. Audited financial disclosures are produced quarterly by public firms in jurisdictions with GAAP-compliant accounting; the application of graph theory on such disclosures is in principle globally replicable. The bookkeeping graph is a primitive of the firm's own economic record, not a derivative of market or text data, and its entropy is the unique scalar summary admitting both axiomatic discipline and structural decomposition by economic activity.

References

Abel, A. B. and J. C. Eberly (1996). Optimal investment with costly reversibility. *Review of Economic Studies* 63(4), 581–593.

Acemoglu, D., V. M. Carvalho, A. Ozdaglar, and A. Tahbaz-Salehi (2012). The network origins of aggregate fluctuations. *Econometrica* 80(5), 1977–2016.

Adelman, M. A. (1969). Comment on the H-concentration measure as a numbers-equivalent. *Review of Economics and Statistics* 51(1), 99–101.

Arya, A., J. C. Fellingham, J. Glover, D. A. Schroeder, and G. Strang (2000). Bookkeeping and reciprocal exchange. *Management Science* 46(2), 193–205.

Bachmann, R., S. Elstner, and E. R. Sims (2013). Uncertainty and economic activity: Evidence from business survey data. *American Economic Journal: Macroeconomics* 5(2), 217–249.

Baker, S. R., N. Bloom, and S. J. Davis (2016). Measuring economic policy uncertainty. *Quarterly Journal of Economics* 131(4), 1593–1636.

Dehmer, M. (2008). Information processing in complex networks: Graph entropy and information functionals. *Applied Mathematics and Computation* 201(1–2), 82–94.

Mowshowitz, A. (1968). Entropy and the complexity of graphs: I. An index of the relative complexity of a graph. *Bulletin of Mathematical Biophysics* 30, 175–204.

Bekaert, G., M. Hoerova, and M. Lo Duca (2013). Risk, uncertainty and monetary policy. *Journal of Monetary Economics* 60(7), 771–788.

Berger, D., I. Dew-Becker, and S. Giglio (2020). Uncertainty shocks as second-moment news shocks. *Review of Economic Studies* 87(1), 40–76.

Bernanke, B. S. (1983). Irreversibility, uncertainty, and cyclical investment. *Quarterly Journal of Economics* 98(1), 85–106.

Bloom, N. (2009). The impact of uncertainty shocks. *Econometrica* 77(3), 623–685.

Bloom, N. (2014). Fluctuations in uncertainty. *Journal of Economic Perspectives* 28(2), 153–176.

Bloom, N., S. Bond, and J. Van Reenen (2007). Uncertainty and investment dynamics. *Review of Economic Studies* 74(2), 391–415.

Bloom, N., M. Floetotto, N. Jaimovich, I. Saporta-Eksten, and S. J. Terry (2018). Really uncertain business cycles. *Econometrica* 86(3), 1031–1065.

Cascaldi-Garcia, D. et al. (2023). What is certain about uncertainty? *Journal of Economic Literature* 61(2), 624–654.

Christiano, L. J., M. Eichenbaum, and C. L. Evans (2005). Nominal rigidities and the dynamic effects of a shock to monetary policy. *Journal of Political Economy* 113(1), 1–45.

Cover, T. M. and J. A. Thomas (2006). *Elements of Information Theory*, 2nd ed. Wiley.

Dechow, P. M., R. G. Sloan, and A. P. Sweeney (1996). Causes and consequences of earnings manipulation. *Contemporary Accounting Research* 13(1), 1–36.

Dixit, A. K. and R. S. Pindyck (1994). *Investment under Uncertainty*. Princeton University Press.

Gulen, H. and M. Ion (2016). Policy uncertainty and corporate investment. *Review of Financial Studies* 29(3), 523–564.

Herskovic, B., B. Kelly, H. Lustig, and S. Van Nieuwerburgh (2016). The common factor in idiosyncratic volatility. *Journal of Financial Economics* 119(2), 249–283.

Herskovic, B. (2018). Networks in production: Asset pricing implications. *Journal of Finance* 73(4), 1785–1818.

Hill, M. O. (1973). Diversity and evenness: A unifying notation and its consequences. *Ecology* 54(2), 427–432.

Im, K. S., M. H. Pesaran, and Y. Shin (2003). Testing for unit roots in heterogeneous panels. *Journal of Econometrics* 115(1), 53–74.

Jones, J. J. (1991). Earnings management during import relief investigations. *Journal of Accounting Research* 29(2), 193–228.

Jurado, K., S. C. Ludvigson, and S. Ng (2015). Measuring uncertainty. *American Economic Review* 105(3), 1177–1216.

Kastner, G. and S. Frühwirth-Schnatter (2014). Ancillarity-sufficiency interweaving strategy (ASIS) for boosting MCMC estimation of stochastic volatility models. *Computational Statistics & Data Analysis* 76, 408–423.

Kim, H. and H. Kung (2017). The asset redeployability channel: How uncertainty affects corporate investment. *Review of Financial Studies* 30(1), 245–280.

Leahy, J. V. and T. M. Whited (1996). The effect of uncertainty on investment: Some stylized facts. *Journal of Money, Credit and Banking* 28(1), 64–83.

Lev, B. (1968). The aggregation problem in financial statements. *Journal of Accounting Research* 6(2), 247–261.

Lev, B. (1970). The informational approach to aggregation in financial statements: Extensions. *Journal of Accounting Research* 8(1), 78–94.

Li, N., P. J. Liang, J. J. Pyo, and G. Zhang (2024). Accounting classification entropy (ACE): Measuring information of accounting classification. Working paper.

Liang, P. J., & Pyo, J. J. (2026a). *AGE & AGER Panel: Accounting Graph Entropy Measures*, Version 1.0 [Data set]. Accounting AI Research Lab, Tepper School of Business, Carnegie Mellon University.

Liang, P. J., & Pyo, J. J. (2026b). *AGE & AGER Panel: Accounting Graph Entropy Measures — Methodology Documentation*, Version 1.0. Accounting AI Research Lab, Tepper School of Business, Carnegie Mellon University.

Liang, P. J. (2026). Three Entropy Measures of Double-Entry Bookkeeping Graph Classification Structure. Working paper, Carnegie Mellon University. Available at `https://www.cmu.edu/tepper/accounting-lab/research/documents/liang2026-06threelaws.pdf`.

Liang, P. J., J. J. Pyo, G. Zhang, and X.-J. Zhang (2026). Accounting Graph Entropy (AGE): Measuring Information of Financial Statement Graph Structure. Working paper, Carnegie Mellon University.

Ludvigson, S. C., S. Ma, and S. Ng (2021). Uncertainty and business cycles: Exogenous impulse or endogenous response? *American Economic Journal: Macroeconomics* 13(4), 369–410.

McDonald, R. and D. Siegel (1986). The value of waiting to invest. *Quarterly Journal of Economics* 101(4), 707–727.

Shannon, C. E. (1948). A mathematical theory of communication. *Bell System Technical Journal* 27, 379–423 and 623–656.

Theil, H. (1969). On the use of information theory concepts in the analysis of financial statements. *Management Science* 15(9), 459–480.

Coase, R. H. (1937). The nature of the firm. *Economica* 4(16), 386–405.

David, J. M. and V. Venkateswaran (2019). The sources of capital misallocation. *American Economic Review* 109(7), 2531–2567.

Grossman, S. J. and O. D. Hart (1986). The costs and benefits of ownership: A theory of vertical and lateral integration. *Journal of Political Economy* 94(4), 691–719.

Hart, O. and J. Moore (1990). Property rights and the nature of the firm. *Journal of Political Economy* 98(6), 1119–1158.

Hsieh, C.-T. and P. J. Klenow (2009). Misallocation and manufacturing TFP in China and India. *Quarterly Journal of Economics* 124(4), 1403–1448.

Lamont, O. (1997). Cash flow and investment: Evidence from internal capital markets. *Journal of Finance* 52(1), 83–109.

Stein, J. C. (1997). Internal capital markets and the competition for corporate resources. *Journal of Finance* 52(1), 111–133.

Alfaro, I., N. Bloom, and X. Lin (2024). The finance uncertainty multiplier. *Journal of Political Economy* 132(2), 577–615.

Ijiri, Y. (1975). *Theory of Accounting Measurement*. American Accounting Association, Studies in Accounting Research No. 10.

Hansen, L. P. and T. J. Sargent (2008). *Robustness*. Princeton University Press.

Sims, C. A. (2003). Implications of rational inattention. *Journal of Monetary Economics* 50(3), 665–690.

Maćkowiak, B. and M. Wiederholt (2009). Optimal sticky prices under rational inattention. *American Economic Review* 99(3), 769–803.

Bernanke, B. and M. Gertler (1989). Agency costs, net worth, and business fluctuations. *American Economic Review* 79(1), 14–31.

Williamson, O. E. (1985). *The Economic Institutions of Capitalism*. Free Press.

Holmström, B. and P. Milgrom (1991). Multitask principal–agent analyses: Incentive contracts, asset ownership, and job design. *Journal of Law, Economics, and Organization* 7, 24–52.

Gilchrist, S. and E. Zakrajšek (2012). Credit spreads and business cycle fluctuations. *American Economic Review* 102(4), 1692–1720.

A Axioms for Edge-entropy measure

Let $\mathcal{G} = (V, E, W)$ denote a directed weighted graph on m nodes, with:

- $V = \{v_1, v_2, \ldots, v_m\}$ the set of nodes, interpreted as accounts in the chart of accounts;
- $E \subseteq V \times V$ the set of directed edges, with e_{ij} representing a journal-entry flow crediting account i and debiting account j;
- $W = (w_{ij}) \in \mathbb{R}^{m \times m}_{\geq 0}$ the weighted adjacency matrix, with $w_{ij} \geq 0$ the cumulative dollar weight of flow from i to j, and $w_{ii} = 0$ for all i (no self-transactions on atomic accounts).

Denote by $\mathcal{W}^0_m$ the set of $m \times m$ non-negative matrices with zero diagonal. Total edge mass is $S(W) = \sum_{i \neq j} w_{ij}$, assumed positive. The normalized edge distribution is $\pi_{ij} = w_{ij}/S(W)$ for $i \neq j$.

A.1 Node-Relabeling and the Domain of Edge Entropy

The chart-of-accounts ordering is an artifact of recordkeeping practice, not informational content: a balance sheet that lists Cash before Receivables conveys the same information as one that lists them in the reverse order. The natural object of analysis is therefore not the matrix W itself but its equivalence class under *simultaneous row-column permutation*—the operation that relabels nodes consistently in both the inflow (column) and outflow (row) dimensions of the adjacency matrix.

Formally, define the equivalence relation $\sim$ on $\mathcal{W}^0_m$ by

$$W \sim W' \quad \Longleftrightarrow \quad \exists\, \sigma \in S_m \text{ such that } w'_{ij} = w_{\sigma(i),\sigma(j)} \text{ for all } i, j.$$

The quotient $\widetilde{\mathcal{W}}^0_m := \mathcal{W}^0_m / \sim$ is the space of node-labeled-up-to-relabeling adjacency matrices.

This is the right domain on which to define entropy measures of the bookkeeping graph for two reasons. First, simultaneous row-column permutation respects the directed structure of journal-entry flows: it preserves which entries lie above the diagonal, which lie below, and which are bilateral. Arbitrary permutation of the $m(m-1)$ off-diagonal cells—which would let one swap w_{ij} with w_{ji} freely—would destroy this directionality and is therefore not an admissible symmetry on the bookkeeping graph. Second, simultaneous row-column permutation is precisely the symmetry generated by node-relabeling: it quotients out the arbitrary chart-of-accounts ordering while preserving every other structural feature.

We therefore frame all subsequent results as statements about functions on $\widetilde{\mathcal{W}}_m^0$, treating node-relabeling invariance as a property of the domain rather than an axiom.

Definition 3 (Shannon edge entropy)**.** For $W \in \mathcal{W}_m^0$ with $S(W) > 0$, the Shannon edge entropy is

$$H_m^{\text{edge}}(W) \;=\; -\sum_{i \neq j} \pi_{ij} \log \pi_{ij}, \tag{16}$$

where the sum is over ordered pairs with $i \neq j$. Throughout Appendix A, log denotes the base-2 logarithm, under which $H_2(1/2, 1/2) = 1$ as required by Axiom 1.

By construction, H_m^{edge} is a function on the quotient $\widetilde{\mathcal{W}}_m^0$: it depends only on the multiset of edge weights, not on the row-column labeling. We do *not* claim invariance under arbitrary permutation of the $m(m-1)$ off-diagonal cells, which would be a stronger and accounting-inadmissible symmetry. The relevant invariance is exactly node-relabeling, built into the domain.

A.2 The Node-Merge Operation and the Grouping Identity

The natural grouping operation in the adjacency-matrix setting is not pairwise merging of edges (which lacks accounting interpretation) but merging of two nodes into one, with the incident edges aggregated accordingly.

Definition 4 (Node-merge, zero-diagonal)**.** For $W \in \mathcal{W}_m^0$ and $a, b \in \{1, \ldots, m\}$ with $a \neq b$, the *node-merge* operation $W \mapsto W^{(a,b)}$ produces a matrix in $\mathcal{W}_{m-1}^0$ as follows. Let c denote the merged node. Then:

$$w_{cj}^{(a,b)} = w_{aj} + w_{bj} \quad \text{for } j \notin \{a, b\}, \tag{17}$$
$$w_{ic}^{(a,b)} = w_{ia} + w_{ib} \quad \text{for } i \notin \{a, b\}, \tag{18}$$
$$w_{ij}^{(a,b)} = w_{ij} \quad \text{for } i, j \notin \{a, b\}, \tag{19}$$
$$w_{cc}^{(a,b)} = 0. \tag{20}$$

The bilateral mass $w_{ab} + w_{ba}$ is eliminated; total edge mass becomes $S' = S(W) - w_{ab} - w_{ba}$.

The zero-diagonal convention $w_{cc}^{(a,b)} = 0$ corresponds to the *intercompany elimination* practice in consolidated financial reporting: transactions between entities that become a single reporting unit post-merger vanish from the consolidated statements.

Define, for the merge $(a,b) \to c$:

$$\begin{aligned} \tau &= \pi_{ab} + \pi_{ba} && \text{(bilateral mass fraction)}, \\ p_j^{\text{out}} &= \pi_{aj} + \pi_{bj} && \text{(row-merge mass for external node } j), \\ p_i^{\text{in}} &= \pi_{ia} + \pi_{ib} && \text{(column-merge mass for external node } i). \end{aligned}$$

We denote by $H_2(x, 1-x) = -x \log x - (1-x)\log(1-x)$ the binary Shannon entropy.

Theorem 2 (Node-merge grouping identity, zero-diagonal)**.** *For any $W \in \mathcal{W}_m^0$ with $S(W) > 0$ and any pair $a \neq b$,*

$$\begin{aligned} H_m^{edge}(W) \;=\; &(1-\tau)\, H_{m-1}^{edge}(W^{(a,b)}) \;+\; H_2(\tau, 1-\tau) \\ &+ \sum_{j \notin \{a,b\}} p_j^{out}\, H_2\Big(\tfrac{\pi_{aj}}{p_j^{out}}, \tfrac{\pi_{bj}}{p_j^{out}}\Big) \\ &+ \sum_{i \notin \{a,b\}} p_i^{in}\, H_2\Big(\tfrac{\pi_{ia}}{p_i^{in}}, \tfrac{\pi_{ib}}{p_i^{in}}\Big) \\ &+ \tau\, H_2\big(\tfrac{\pi_{ab}}{\tau}, \tfrac{\pi_{ba}}{\tau}\big)\,. \end{aligned} \tag{21}$$

Proof. Partition the $m(m-1)$ off-diagonal cells of W into four disjoint classes:

1. *Untouched external cells*: (i,j) with $i, j \notin \{a,b\}$ and $i \neq j$. These pass through the merge unchanged.
2. *Row-merge pairs*: for each $j \notin \{a,b\}$, the pair $\{(a,j),(b,j)\}$ collapses to a single cell (c,j) of mass p_j^{out}.
3. *Column-merge pairs*: for each $i \notin \{a,b\}$, the pair $\{(i,a),(i,b)\}$ collapses to a single cell (i,c) of mass p_i^{in}.
4. *Bilateral pair*: $\{(a,b),(b,a)\}$, which is *removed* from the distribution under the zero-diagonal convention.

For any partition of a probability distribution $\{\pi_k\}$ into groups $G_1, \dots, G_K$ with group masses $P_\ell = \sum_{k \in G_\ell} \pi_k$, the standard grouping identity gives

$$-\sum_k \pi_k \log \pi_k \;=\; -\sum_\ell P_\ell \log P_\ell \;+\; \sum_\ell P_\ell \left(-\sum_{k \in G_\ell} \tfrac{\pi_k}{P_\ell} \log \tfrac{\pi_k}{P_\ell} \right). \tag{22}$$

Apply (22) with the four classes above as groups. The first term on the right-hand side of (22) is

$$-\sum_{i,j \notin \{a,b\}, i \neq j} \pi_{ij} \log \pi_{ij} \;-\; \sum_{j \notin \{a,b\}} p_j^{\text{out}} \log p_j^{\text{out}} \;-\; \sum_{i \notin \{a,b\}} p_i^{\text{in}} \log p_i^{\text{in}} \;-\; \tau \log \tau.$$

The within-group entropy terms for row-merge, column-merge, and bilateral classes are binary entropies multiplied by their respective masses (classes with singleton groups contribute zero).

Using the post-merge renormalization $\pi_{ij}^{(a,b)} = \pi_{ij}/(1-\tau)$ for external cells and $\pi_{cj}^{(a,b)} = p_j^{\text{out}}/(1-\tau)$, $\pi_{ic}^{(a,b)} = p_i^{\text{in}}/(1-\tau)$, one can verify

$$H_{m-1}^{\text{edge}}(W^{(a,b)}) \;=\; \frac{1}{1-\tau}\left[-\sum_{i,j\notin\{a,b\},i\neq j}\pi_{ij}\log\pi_{ij} - \sum_j p_j^{\text{out}}\log p_j^{\text{out}} - \sum_i p_i^{\text{in}}\log p_i^{\text{in}}\right] + \log(1-\tau).$$

Multiplying by $(1-\tau)$ and using the identity $-\tau\log\tau = H_2(\tau,1-\tau)+(1-\tau)\log(1-\tau)$ (immediate from $H_2(\tau,1-\tau) = -\tau\log\tau-(1-\tau)\log(1-\tau)$) gives, after simplification, the claimed identity. (The algebra is straightforward; the key step is the bookkeeping of the $\log(1-\tau)$ terms.) $\square$

A.3 Axiomatic Characterization

We now consider an arbitrary sequence of functions $\{J_m\}_{m\geq 2}$, where each $J_m : \widetilde{\mathcal{W}}_m^0 \to \mathbb{R}$ assigns a real number to each node-relabeling-equivalence class of zero-diagonal adjacency matrices, and ask: under what axioms must J_m coincide with H_m^{edge}?

Because the domain $\widetilde{\mathcal{W}}_m^0$ is the quotient under simultaneous row-column permutation, node-relabeling invariance is built into the formulation rather than imposed as a separate axiom. This parallels the Faddeev (1956) treatment of the classical case, in which entropy is defined on the space of probability distributions on m atoms (rather than on ordered tuples in $\mathbb{R}^m$), so that symmetry is a property of the domain rather than an axiom about the function. The Cover and Thomas (2006) presentation derives symmetry from the grouping axiom; we adopt the cleaner Faddeev convention because it isolates more sharply the axiom that does the substantive work—the grouping axiom—from the structural choice of domain.

The Axioms The axioms are stated in the body as Axioms 1–3 (inside Theorem 1); we restate the symbol $J_2^{\text{bin}}(x) := J_2(\pi)$ for reference, where π is the two-edge distribution with probabilities x and $1-x$. (On $\widetilde{\mathcal{W}}_2^0$, the two off-diagonal cells are exchanged by node-relabeling, so $J_2^{\text{bin}}(x) = J_2^{\text{bin}}(1-x)$ automatically.)

Three remarks on Axioms 1–3.

First, the axiomatization is structurally parallel to Faddeev's: normalization, continuity, and a single grouping axiom. Cover and Thomas's monotonicity axiom is replaced by node-merge grouping, which is stronger.

Second, no symmetry axiom appears in the list. Node-relabeling invariance is built into the domain; no further symmetry between row-cells and column-cells, or between π_{ij} and π_{ji}, is imposed. This is essential: imposing such a symmetry on the matrix would conflate the credit side with the debit side at the matrix-cell level, foreclosing on debit-credit duality as a substantive constraint on the entropy measure.

Third, the single-function clause of Axiom 3 is stated for definiteness. In principle, one could admit four distinct binary functions—$\phi_{\text{bil}}, \phi_{\text{row}}, \phi_{\text{col}}, \phi_{\text{base}}$—in the four roles and still obtain a well-defined grouping rule. One might therefore expect the single-function clause to carry substantive axiomatic content, specifically encoding debit-credit duality at the axiom level.

A Sufficient-Determination Lemma The following lemma separates two tasks in the uniqueness argument: pinning down the functional form of J_2^{bin}, and propagating that determination to J_m on the full domain $\widetilde{\mathcal{W}}_m^0$. It is valid for any J_2^{bin}, not just H_2.

Lemma 3 (Sufficiency of J_2^{bin})**.** *Suppose $\{J_m\}_{m\geq 2}$ satisfies Axioms 1, 2, 3, and suppose $J_2^{bin} : (0,1) \to \mathbb{R}$ is determined. Then $J_m(W)$ is determined for every $m \geq 2$ and every $W \in \widetilde{\mathcal{W}}_m^0$ with $S(W) > 0$.*

Proof. Induction on m.

Base ($m = 2$). For $W \in \widetilde{\mathcal{W}}_2^0$, the edge distribution is $(x, 1-x)$ for some $x \in (0,1)$, and $J_2(W) = J_2^{\text{bin}}(x)$ by the definition of J_2^{bin}. Determined.

Inductive step ($m > 2$). Fix $W \in \widetilde{\mathcal{W}}_m^0$ with $S(W) > 0$, and choose any pair $a \neq b$. By Axiom 3:

$$J_m(W) = (1-\tau)\, J_{m-1}(W^{(a,b)}) + J_2^{\text{bin}}(\tau) + \sum_{j\notin\{a,b\}} p_j^{\text{out}}\, J_2^{\text{bin}}\Big(\tfrac{\pi_{aj}}{p_j^{\text{out}}}\Big) + \sum_{i\notin\{a,b\}} p_i^{\text{in}}\, J_2^{\text{bin}}\Big(\tfrac{\pi_{ia}}{p_i^{\text{in}}}\Big) + \tau\, J_2^{\text{bin}}\big(\tfrac{\pi_{ab}}{\tau}\big)\,.$$

By the inductive hypothesis, $J_{m-1}(W^{(a,b)})$ is determined. Every evaluation of J_2^{bin} on the right-hand side is at an explicit argument in $(0,1)$ and is therefore determined by hypothesis. Hence $J_m(W)$ is determined. $\square$

Remark 1 (Consistency of Axiom 3)*.* Axiom 3 prescribes a value for $J_m(W)$ for each choice of pair (a,b). For Axiom 3 to be satisfiable at all, all pair choices must prescribe the same value. This consistency is guaranteed once $J_2^{\text{bin}} = H_2$ by Theorem 2, which establishes that H_m^{edge} satisfies the identity for every (a,b). The Sufficiency Lemma therefore determines $J_m(W)$ consistently: the right-hand side of Axiom 3, evaluated with $J_2^{\text{bin}} = H_2$ and with $J_{m-1} = H_{m-1}^{\text{edge}}$ by induction, equals $H_m^{\text{edge}}(W)$ independent of the pair choice.

Proof of Theorem 1. The proof proceeds in three steps: (i) derive a functional equation on J_2^{bin} by applying Axiom 3 to a three-node family in two distinct ways; (ii) solve the functional equation using Axioms 1 and 2; (iii) apply Lemma 3 to extend the determination to all of $\widetilde{\mathcal{W}}_m^0$.

Step 1: Functional equation from $m = 3$. We derive the functional equation on the direction-symmetric 3-node family $\pi_{ij} = \pi_{ji}$. The restriction to this family is a dimensional convenience, not an accounting commitment: the family's 2-parameter freedom matches the argument dimensionality of the Faddeev equation, and its direction-symmetry causes the recursive-base and within-bilateral arguments to land at 1/2, where normalization immediately fixes them. The accounting content—debit-credit duality—does not enter at this step; it enters through the domain's node-relabeling invariance.Lemma 3 establishes that the determination of J_2^{bin} via the symmetric-family equation extends to J_m on all $W \in \widetilde{\mathcal{W}}_m^0$, symmetric or not.

Consider the three-node family parameterized by $(a, b, c) \in \mathbb{R}^3_{\geq 0}$ with $2a + 2b + 2c = 1$, defined by

$$\pi_{12} = \pi_{21} = a, \quad \pi_{13} = \pi_{31} = b, \quad \pi_{23} = \pi_{32} = c.$$

Merging $\{2, 3\}$*:* $\tau = 2c$, $p_1^{\mathrm{out}} = a + b$, $p_1^{\mathrm{in}} = a + b$. The post-merge graph has two edges with probabilities $(a + b)/(a + b) = 1/2$ each after renormalization (by symmetry $p_1^{\mathrm{out}} = p_1^{\mathrm{in}}$ and $1 - 2c = 2(a + b)$), so $J_2^{\mathrm{post}} = J_2^{\mathrm{bin}}(1/2) = 1$ by Axiom 1. The bilateral split is $c/(2c) = 1/2$, giving binary $J_2^{\mathrm{bin}}(1/2) = 1$.

Applying Axiom 3:

$$J_6(\pi) = H_2(2c, 1 - 2c) \cdot \mathbf{1} + (1 - 2c) \cdot 1 + 2(a + b)\, J_2^{\mathrm{bin}}\Big(\tfrac{a}{a+b}\Big) + 2c \cdot 1, \tag{23}$$

where H_2 here denotes the *known* binary function induced by Axiom 3—which, by the single-function requirement, coincides with J_2^{bin}. Write $\phi := J_2^{\mathrm{bin}}$ (treating ϕ as a function of a single argument in $(0, 1)$, with $\phi(x) = \phi(1 - x)$ by symmetry).

Merging $\{1, 2\}$*:* $\tau' = 2a$, analogous computation gives

$$J_6(\pi) = \phi(2a) + (1 - 2a) \cdot 1 + 2(b + c)\, \phi\Big(\tfrac{b}{b+c}\Big) + 2a \cdot 1. \tag{24}$$

Equating (23) and (24) and simplifying (using $a + b + c = 1/2$):

$$\phi(2c) + (1 - 2c)\, \phi\Big(\tfrac{a}{a+b}\Big) \;=\; \phi(2a) + (1 - 2a)\, \phi\Big(\tfrac{b}{b+c}\Big). \tag{25}$$

Substitute $x := 2a, y := 2c$, so $a = x/2, c = y/2, b = (1 - x - y)/2$. Then $a/(a + b) = x/(1 - y)$ and $b/(b + c) = (1 - x - y)/(1 - x)$. Using $\phi(1 - z) = \phi(z)$, $\phi((1 - x - y)/(1 - x)) = \phi(y/(1 - x))$. Equation (25) becomes

$$\phi(y) + (1 - y)\, \phi\Big(\tfrac{x}{1-y}\Big) \;=\; \phi(x) + (1 - x)\, \phi\Big(\tfrac{y}{1-x}\Big), \tag{26}$$

valid for all (x, y) with $x, y > 0$ and $x + y < 1$. As (a, b, c) range over the open 2-simplex, the substitutions $x = 2a, y = 2c$ range over the full open triangle $\{(x, y) : x, y > 0, x + y < 1\}$, which is the standard domain of Faddeev's equation.

Step 2: Solve (26). Equation (26) is Faddeev's (1956) fundamental functional equation for binary entropy. The unique continuous solution satisfying $\phi(1/2) = 1$ and $\phi(x) = \phi(1 - x)$ is

$$\phi(x) \;=\; -x \log x - (1 - x) \log(1 - x) \;=\; H_2(x, 1 - x).$$

A standard reference is Aczél and Daróczy (1975), Chapter 3. The argument reduces (26) to the

Cauchy equation $f(xy) = f(x) + f(y)$ via the substitution $f(x) = -\phi(x) - \phi(1-x)$ on the domain where both arguments are in $(0,1)$, together with continuity.

Step 3: Extend to $m \geq 2$ via the Sufficiency Lemma. By Step 2, $J_2^{\mathrm{bin}} = H_2$ on $(0,1)$. Apply Lemma 3: $J_m(W)$ is determined for every $m \geq 2$ and every $W \in \widetilde{\mathcal{W}}_m^0$.

To identify the determined value as $H_m^{\mathrm{edge}}(W)$, proceed by induction. For $m = 2$: $J_2(W) = J_2^{\mathrm{bin}}(\pi_{12}) = H_2(\pi_{12}) = H_2^{\mathrm{edge}}(W)$ directly. For $m > 2$: the inductive hypothesis $J_{m-1} = H_{m-1}^{\mathrm{edge}}$ together with $J_2^{\mathrm{bin}} = H_2$ makes the right-hand side of Axiom 3's identity coincide arithmetically with the right-hand side of Theorem 2's identity applied to $H_m^{\mathrm{edge}}(W)$. By the consistency of Axiom 3 (guaranteed by Theorem 2 as satisfiability witness), either side equals $H_m^{\mathrm{edge}}(W)$. Hence $J_m(W) = H_m^{\mathrm{edge}}(W)$ for all m and all W. This completes the proof. $\square$

B Proof of Proposition 1

Proof of Proposition 1: Fix firm i and quarter t and suppress the $_{it}$ subscript throughout the proof. The bookkeeping graph has edge set $\mathcal{E}$ partitioned as $\mathcal{E} = \bigsqcup_{s \in \mathcal{S}} \mathcal{E}^{(s)}$. For each edge $e \in \mathcal{E}$ let $w(e)$ denote its weight, let $W^{(s)} \equiv \sum_{e \in \mathcal{E}^{(s)}} w(e)$, and $W \equiv \sum_{e \in \mathcal{E}} w(e) = \sum_{s \in \mathcal{S}} W^{(s)}$. The subgraph weight share is $\omega^{(s)} \equiv W^{(s)}/W$, with $\sum_{s \in \mathcal{S}} \omega^{(s)} = 1$.

By Definition 2,

$$H \;=\; -\sum_{e \in \mathcal{E}} \frac{w(e)}{W} \log \frac{w(e)}{W}.$$

The within-subgraph entropy is

$$H^{(s)} \;=\; -\sum_{e \in \mathcal{E}^{(s)}} \frac{w(e)}{W^{(s)}} \log \frac{w(e)}{W^{(s)}},$$

and the between-subgraph entropy is

$$H^{(\mathcal{S})} \;=\; -\sum_{s \in \mathcal{S}} \omega^{(s)} \log \omega^{(s)}.$$

Identity (6) follows from the partition of $\mathcal{E}$ together with $\log(ab) = \log a + \log b$:

$$\begin{aligned}
H &= -\sum_{s\in\mathcal{S}} \sum_{e\in\mathcal{E}^{(s)}} \frac{w(e)}{W} \log \frac{w(e)}{W} \\
&= -\sum_{s\in\mathcal{S}} \omega^{(s)} \sum_{e\in\mathcal{E}^{(s)}} \frac{w(e)}{W^{(s)}} \log\left(\frac{w(e)}{W^{(s)}} \cdot \omega^{(s)}\right) \\
&= -\sum_{s\in\mathcal{S}} \omega^{(s)} \sum_{e\in\mathcal{E}^{(s)}} \frac{w(e)}{W^{(s)}} \left[\log \frac{w(e)}{W^{(s)}} + \log \omega^{(s)}\right] \\
&= \sum_{s\in\mathcal{S}} \omega^{(s)} H^{(s)} \; - \; \sum_{s\in\mathcal{S}} \omega^{(s)} \log \omega^{(s)} \\
&= H^{(\mathcal{S})} + \sum_{s\in\mathcal{S}} \omega^{(s)} H^{(s)}. \quad \square
\end{aligned}$$

Re-attaching the $_{it}$ subscripts on every symbol recovers Proposition 1 verbatim.

C Empirical Properties of Financial-Statement Entropy

This section organizes the empirical evidence under five criteria that any input to the JLN factor-augmented stochastic-volatility estimator should satisfy: (i) *stationarity*, so that conditional volatility is well-defined; (ii) *forecastability*, so that Stage 1 has predictable variation to absorb; (iii) *business-cycle-relevant frequency content*, so that the Stage 2 stochastic-volatility innovations carry macroeconomic content; (iv) *conditional heteroskedasticity*, so that stochastic volatility is the appropriate filter; and (v) *economic interpretability*, so that filter output admits structural reading. The four entropy series satisfy each criterion, and the cross-correlation and cross-channel analyses below establish that the four readings carry distinct information.

The role of economy-wide drivers of financial-statement entropy. Movement in the entropy series has two distinct origins: (i) firm-level reallocation across the bookkeeping channels during each quarter—within-firm redeployment of cash, working-capital, value-creation, and financing flows—which is the structural object H_{it} is designed to read; and (ii) economy-wide changes in accounting standards that mechanically alter every firm's bookkeeping graph contemporaneously and are visible in Figure 6 as common-to-all-firms regime shifts.[12] Neither is the final variable of inter-

[12]The clearest example in our sample is the introduction of Other Comprehensive Income (OCI) reporting under SFAS 130, effective for fiscal years beginning after December 15, 1997. The standard requires firms to report unrealized items such as foreign-currency translation adjustments, certain pension adjustments, and available-for-sale securities mark-to-market outside net income, which translates into a new income-statement node and its incident edges entering every reporting firm's bookkeeping graph. The IS- and operating-subgraph regime shifts visible in Figure 6 around 2001–2002 are consistent with the consolidation of OCI presentation practice across the panel, though precise dating is complicated by staggered firm-level adoption and by overlapping reforms in the same window (e.g., SFAS 141/142 on business combinations and goodwill in 2001). The construction logic is identical for any such rule change: a new GAAP-required node or edge enters every firm's graph at once, the cross-sectional π-distribution is mechanically reshaped, and the resulting movement in $\bar{H}_t^{(\cdot)}$ is common to all firms and predictable from the calendar—exactly the kind of variation Stage 1 of the JLN filter is designed to absorb.

est. The Entropic Uncertainty Index is the time-varying conditional volatility of the *unforecastable* component of H_{it}, extracted by the JLN filter of Section 4.1: Stage 1 absorbs aggregate, predictable variation—including secular shifts driven by accounting-standard rollouts—into factor loadings and lags; Stage 2 reads the conditional heteroskedasticity of the residual. Expected movements in H_{it}, economic or rule-driven, therefore do not enter the final index.

Distributional properties. Figure 6 plots the four equal-weighted cross-sectional means $\bar{H}_t^{(\cdot)} \equiv N_t^{-1} \sum_{i \in \mathcal{S}_t} H_{it}^{(\cdot)}$ over the 1990Q1–2011Q2 window. The four series exhibit distinct profiles: total entropy spikes sharply in 2002; operating-subgraph entropy undergoes a regime shift in 2001Q2 that persists through the end of the sample; income-statement entropy rises contemporaneously with both the 2001 and the 2007–2009 recessions and reaches its sample peak in 2009; financing-subgraph entropy shows a permanent level shift in 2001–2002. Figure 7 complements the cross-sectional means with the corresponding firm-quarter distribution: the equal-weighted mean (solid), the cross-sectional median (dashed), and the inter-decile and inter-quartile bands across the panel of 123 firms. Two facts visible in the IQR figure are worth emphasizing. First, the firm-quarter distribution is wide relative to the cross-sectional mean—for example, the inter-decile spread of H_{it}^{Tot} is roughly 0.87 around a cross-sectional mean of 2.13—so the macroeconomic series plotted in Figure 6 is one moment of a substantially heterogeneous panel. Second, the IQR bands themselves move at business-cycle frequencies: the cross-sectional dispersion of H_{it}^{IS} widens visibly during the 2008–2009 contraction, anticipating the formal heteroskedasticity tests reported below.

Table 15 reports unified summary statistics both at the firm-quarter level (the input to the Stage 1 forecasting regression) and at the cross-sectional-mean level (a useful diagnostic). Two features of the levels deserve note. First, the implied effective number of channels $\exp(\bar{H})$, the perplexity interpretation of entropy, varies substantially across subgraphs: roughly 8.4 effective channels in the full graph, against 5.0 in the financing subgraph, 3.2 in the income-statement subgraph, and 2.3 in the operating subgraph. The operating subgraph's low effective dimensionality reflects its concentrated economic content—two edges (CFO–ΔNNCA and CFI–ΔNNCA) carry the bulk of operating activity for a typical firm-quarter—while the financing subgraph's higher dimensionality reflects firms' use of multiple instruments (debt issuance, repurchases, dividend payout, equity transactions) at distinct intensities each quarter. Cross-firm dispersion is economically meaningful: the firm-quarter perplexity of the total graph has a 5th–95th percentile range of 4.8–14.3, indicating that some firms operate with effectively five distinct channels of economic activity per quarter while others operate with fourteen.

A central feature of the construction is that the level of entropy is itself structural information about the firm: a firm operating through more concentrated channels has a lower H_{it} than one operating through more diffuse channels. The conditional volatility of H_{it}, which is what the JLN filter ultimately extracts, is therefore an intrinsically scaled object: each firm's entropy moves within its own construction-based support $H_{it} \in [0, \log |\mathcal{E}_{it}|]$, so a one-standard-deviation conditional movement measures the typical reorganization of the firm's effective channel distribution as

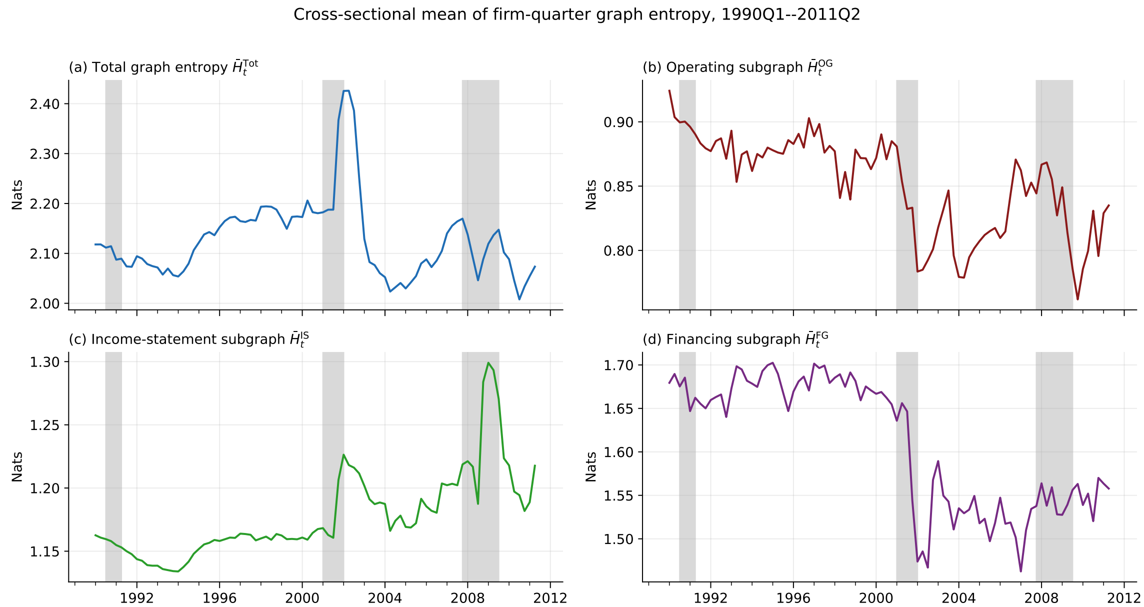

Figure 6: Time series of cross-sectional mean entropy, 1990Q1–2011Q2. Equal-weighted cross-sectional means of firm-quarter entropies across $N = 123$ firms in the balanced panel: (a) total graph entropy $\bar{H}_t^{\mathrm{Tot}}$, (b) operating-subgraph entropy $\bar{H}_t^{\mathrm{OG}}$, (c) income-statement-subgraph entropy $\bar{H}_t^{\mathrm{IS}}$, (d) financing-subgraph entropy $\bar{H}_t^{\mathrm{FG}}$. Shaded vertical bands indicate NBER recessions (1990Q3–1991Q1, 2001Q1–2001Q4, 2007Q4–2009Q2). The four series exhibit distinct profiles: total entropy spikes sharply in 2002; operating-subgraph entropy undergoes a regime shift in 2001Q2 that persists through the end of the sample; income-statement entropy rises contemporaneously with recessions and reaches its sample peak in 2009; financing-subgraph entropy shows a permanent level shift in 2001–2002. Source: authors' calculations on Compustat North America quarterly fundamentals.

Table 15: Summary Statistics for Entropy Series

	Mean	$\exp(\bar{H})$	SD	P10	P50	P90	Skew	Kurt.
Panel A. Firm-quarter level ($N \times T = 10{,}578$)								
H_{it}^{Tot}	2.128	8.40	0.327	1.691	2.133	2.557	−0.056	−0.441
H_{it}^{OG}	0.851	2.34	0.192	0.584	0.930	0.998	−1.907	3.510
H_{it}^{IS}	1.178	3.25	0.089	1.078	1.166	1.291	1.077	2.911
H_{it}^{FG}	1.610	5.00	0.237	1.302	1.650	1.868	−1.376	3.845
Panel B. Cross-sectional mean $\bar{H}_t$ ($T = 86$)								
$\bar{H}_t^{\mathrm{Tot}}$	2.128	8.40	0.081	2.049	2.116	2.191	1.722	4.080
$\bar{H}_t^{\mathrm{OG}}$	0.851	2.34	0.038	0.795	0.863	0.891	−0.522	−0.798
$\bar{H}_t^{\mathrm{IS}}$	1.178	3.25	0.035	1.142	1.164	1.218	1.501	2.578
$\bar{H}_t^{\mathrm{FG}}$	1.610	5.00	0.075	1.518	1.647	1.691	−0.308	−1.498

Notes: Panel A reports descriptive statistics over 10,578 firm-quarter observations across 123 firms and 86 quarters (1990Q1–2011Q2). Panel B reports descriptive statistics of the equal-weighted cross-sectional mean $\bar{H}_t^{(\cdot)}$ over $T = 86$ quarters. $\exp(\bar{H})$ is the implied effective number of edges (perplexity).

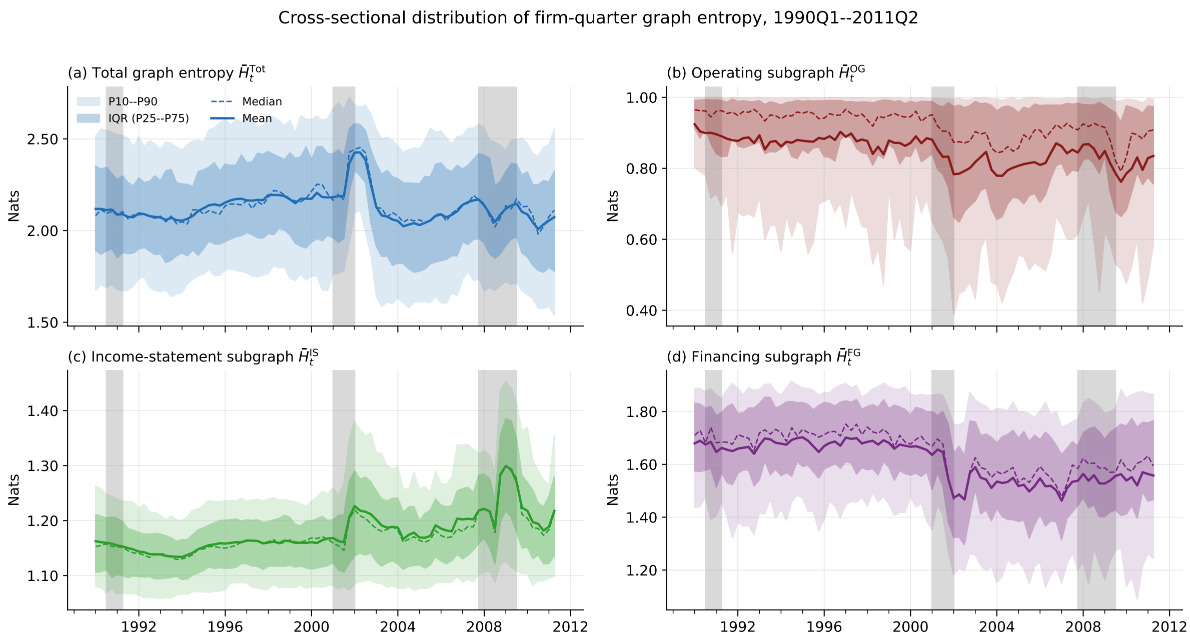

Figure 7: Cross-sectional distribution of firm-quarter entropies, 1990Q1–2011Q2. For each of the four entropy series, the figure plots the equal-weighted cross-sectional mean (solid), the cross-sectional median (dashed black), the inter-quartile band (P25–P75, dark shading), and the inter-decile band (P10–P90, light shading) across the panel of $N = 123$ firms in each quarter. The bands display the heterogeneity that the cross-sectional means in Figure 6 aggregate over: cross-sectional dispersion is substantial relative to the mean, time-varying, and widens during NBER recessions for the income-statement and financing subgraphs. Shaded vertical bands indicate NBER recessions.

a fraction of its own structural capacity. A movement of this size therefore carries comparable structural meaning across a small firm with five effective channels and a large firm with fourteen, even though absolute entropy levels and absolute bounds differ.

Variance decomposition: where does the variation come from? Table 16 decomposes total panel variance into between-firm and within-firm components. Between-firm variation captures structural heterogeneity—the cross-section of business models—while within-firm variation captures temporal evolution of each firm's structural state. Both matter for our purposes, but for distinct reasons: between-firm variation establishes that the construction discriminates across firms, while within-firm variation is the substrate of the JLN filter (the filter extracts conditional volatility within firms after the Stage 1 forecasting regression removes the firm-specific mean). The decomposition shows that within-firm variation is the dominant component for the operating (87%), financing (81%), and income-statement (57%) subgraphs, while the total graph splits roughly evenly (53% / 47%). The time-series content the filter is designed to exploit is most of the variation in three of the four series and a substantial share even in the fourth.

Table 16: Variance Decomposition: Between-Firm vs. Within-Firm

	Total Var.	Between	Within	σ_b	σ_w
H_{it}^{Tot}	0.107	53.0%	47.0%	2.213	0.225
H_{it}^{OG}	0.037	12.9%	87.1%	0.643	0.181
H_{it}^{IS}	0.008	43.0%	57.0%	0.544	0.068
H_{it}^{FG}	0.056	18.6%	81.4%	0.951	0.215

Notes: Within-firm and between-firm shares of total panel variance, computed as SS_w/SS_T and SS_b/SS_T respectively. σ_b and σ_w are the corresponding between-firm and within-firm standard deviations.

Stationarity. Conditional volatility is well-defined only for stationary processes, so the first inferential question is whether the entropy series are stationary. Table 17 reports four complementary tests. At the aggregate level, augmented Dickey–Fuller tests fail to reject a unit root at conventional levels ($p = 0.02$–0.51), but the cross-sectional means are highly persistent (AR(1) coefficients of 0.86–0.94), so power against persistent stationary alternatives is low in $T = 86$ samples; KPSS tests do not reject stationarity for $\bar{H}_t^{\text{Tot}}$ (the most direct counterpart to JLN's profit-based input, i.e., firm-level quarterly profit growth as used in Jurado et al., 2015); and variance-ratio statistics $VR(8) < 1$ for $\bar{H}_t^{\text{OG}}$ (0.55) and $\bar{H}_t^{\text{FG}}$ (0.56), the signature of mean-reversion at horizons relevant to the filter rather than random-walk behavior.

The decisive test is the panel unit root test of Im et al. (2003) (IPS), which exploits the cross-sectional dimension to gain power. The IPS test rejects the null of a unit root in every panel at the 1% level. Equivalently, individual-firm ADF tests reject the null of a unit root at 5% for between 36% and 91% of the firms in the panel. Together with the construction-based bound

$H_{it} \in [0, \log |\mathcal{E}_{it}|]$, which rules out long-run divergence, the evidence is consistent with a persistent stationary process. Block-bootstrap 95% confidence intervals on the aggregate AR(1) coefficients are $[0.709, 0.950]$, $[0.678, 0.917]$, $[0.735, 0.949]$, and $[0.757, 0.970]$ for the Total, OG, IS, and FG series respectively, all bounded away from unity. This profile—high autocorrelation with bounded support—is exactly the profile the JLN factor-augmented forecasting regression of Section 4.1 is designed to handle: Stage 1 absorbs the predictable persistence through lags, common factors, and macro/financial controls; the residual is the unforecastable component the Stage 2 stochastic-volatility filter then characterizes.

Table 17: Persistence and Stationarity of the Entropy Series

	Aggregate ($T = 86$)		Aggregate Tests		Panel-Level Tests		
	AR(1)	Half-life	ADF p	KPSS p	IPS p	$\bar{t}_i$	% reject
$\bar{H}_t^{\mathrm{Tot}}$	0.911	7.41	0.017	≥ 0.10	< 0.001	-3.36	73.2%
$\bar{H}_t^{\mathrm{OG}}$	0.858	4.52	0.151	≤ 0.01	< 0.001	-3.88	91.1%
$\bar{H}_t^{\mathrm{IS}}$	0.908	7.20	0.303	≤ 0.01	< 0.001	-2.65	35.8%
$\bar{H}_t^{\mathrm{FG}}$	0.937	10.70	0.514	≤ 0.01	< 0.001	-3.53	73.2%

Notes: AR(1) coefficients are estimated by OLS on the quarterly cross-sectional means; half-life is $\log(0.5)/\log|\mathrm{AR}(1)|$ in quarters. ADF and KPSS p-values are for the aggregate cross-sectional means. IPS is the Im et al. (2003) panel unit root test computed from individual ADF t-statistics; $\bar{t}_i$ is the cross-sectional mean of the firm-level ADF t-statistics; "% reject is the share of firms for which the firm-level ADF test rejects the unit-root null at the 5% level.

Forecastability: predictable persistence and Stage 1 leverage. The JLN filter's Stage 1 separates predictable from unpredictable variation, and its Stage 2 characterizes the volatility of the unpredictable component. For the filter to produce informative output, the input must be substantially forecastable: if there were no predictable persistence, Stage 1 would have nothing to remove and the volatility filter would simply track the input's own volatility. Firm-by-firm AR(4) regressions yield mean within-firm R^2 of 0.38 (operating subgraph), 0.36 (financing subgraph), 0.63 (total graph), and 0.68 (income-statement subgraph), with substantial cross-firm heterogeneity (10th–90th percentile ranges from 0.14 to 0.86 across series). At the within-firm level, 40–70% of period-to-period variation is predictable from own lags alone—before the JLN factor structure and macro/financial controls are added. This level of forecastability is sufficient for Stage 1 to do meaningful work and substantially exceeds the forecastability of profit growth in JLN's firm-level sample (Jurado et al., 2015, Table 6), where comparable AR(4) projections deliver mean within-firm R^2 below 0.20.

Conditional heteroskedasticity. Stochastic volatility is the appropriate Stage 2 model only if the data exhibit conditional heteroskedasticity: time-varying conditional variance is what the filter extracts. We test for ARCH effects in the residuals from firm-level AR(1) regressions. At the firm level, ARCH-LM tests with four lags reject the null of constant conditional variance for 49% of firms in the income-statement panel, 33% in the operating panel, 21% in the total-graph panel, and 15% in the financing panel. At the aggregate (cross-sectional mean) level, the financing-subgraph series exhibits significant ARCH effects (LM $= 14.9$, $p = 0.005$); the other series have weaker but still positive evidence of conditional heteroskedasticity, consistent with the aggregation reducing idiosyncratic ARCH variation. Two implications follow. First, the SV filter is not over-fitting: genuine conditional heteroskedasticity exists in the data, and the filter's output reflects it. Second, the cross-sectional dispersion of ARCH evidence—49% of IS firms but only 15% of FG firms—suggests that channel-specific heterogeneity in volatility dynamics is itself substantive, not noise: a finding that motivates the structured uncertainty index of Section 3.4.

Frequency-domain content. The JLN filter's output is the conditional volatility of the unpredictable component of the input. For this output to be business-cycle-relevant, the input itself must carry variation at business-cycle frequencies. Table 18 reports the share of variance falling in three frequency bands: high-frequency (< 6 quarters), business-cycle (6–32 quarters), and low-frequency (> 32 quarters). The business-cycle share is 57% for $\bar{H}_t^{\mathrm{Tot}}$, 44% for $\bar{H}_t^{\mathrm{OG}}$, 34% for $\bar{H}_t^{\mathrm{IS}}$, and 15% for $\bar{H}_t^{\mathrm{FG}}$. By comparison, the same band typically captures under thirty percent of asset-price variance and twenty percent of return variance. Structural reorganization of the firm, as recorded in the bookkeeping graph, moves at business-cycle frequencies; the resulting filtered uncertainty series should inherit business-cycle-relevant variation, which they do (Section 4.3). The financing subgraph, with 15% of its variance in the business-cycle band but 82% at low frequencies, exhibits structural variation on a slower timescale: the post-2001 level shift visible in Figure 6(d) reflects a permanent reorganization of corporate financing patterns rather than a business-cycle fluctuation, and the JLN filter correctly assigns the level shift to the predictable Stage 1 component, leaving cyclical fluctuation around it as the source of filtered uncertainty.

Table 18: Spectral Variance Decomposition (Frequency Bands)

	High-freq. (< 6q)	Business-cycle (6–32q)	Low-freq. (> 32q)
$\bar{H}_t^{\mathrm{Tot}}$	2.4%	56.7%	40.8%
$\bar{H}_t^{\mathrm{OG}}$	8.5%	44.0%	47.5%
$\bar{H}_t^{\mathrm{IS}}$	6.3%	34.3%	59.4%
$\bar{H}_t^{\mathrm{FG}}$	3.8%	14.6%	81.7%

Notes: Periodogram-based decomposition of variance (series demeaned). The business-cycle band corresponds to fluctuations with periods of 6 to 32 quarters, the conventional NBER cycle frequencies.

Channel-specific co-movement. Table 19 reports contemporaneous correlations among the four aggregate series under both the cross-sectional-mean (CSA) and the principal-component (PCA) aggregation schemes, plus the median across firms of within-firm first-difference correlations. Three patterns are economically informative.

Table 19: Contemporaneous Correlations Among Entropy Series

	Total	OG	IS	FG
Panel A. Cross-sectional mean (CSA) aggregation				
$\bar{H}_t^{\text{Tot}}$	1.000			
$\bar{H}_t^{\text{OG}}$	−0.022	1.000		
$\bar{H}_t^{\text{IS}}$	0.208	−0.561	1.000	
$\bar{H}_t^{\text{FG}}$	−0.015	0.755	−0.708	1.000
Panel B. First-principal-component (PCA) aggregation				
PC_1^{Tot}	1.000			
PC_1^{OG}	0.183	1.000		
PC_1^{IS}	0.059	−0.634	1.000	
PC_1^{FG}	0.148	0.820	−0.758	1.000
Panel C. Within-firm first-difference correlations (median across firms)				
$\Delta H_{it}^{\text{Tot}}$	1.000			
$\Delta H_{it}^{\text{OG}}$	0.020	1.000		
$\Delta H_{it}^{\text{IS}}$	0.213	−0.022	1.000	
$\Delta H_{it}^{\text{FG}}$	0.256	−0.044	−0.042	1.000

Notes: Panels A and B compute correlations on the $T = 86$ quarterly time series. Panel C reports the median across the $N = 123$ firms of within-firm correlations of first differences. CSA aggregation is the equal-weighted cross-sectional mean; PCA aggregation is the first principal component of the firm-level standardized panel.

First, the three subgraphs are mutually correlated in directions consistent with the substitution structure that double-entry bookkeeping imposes across flow margins. The operating and financing subgraphs comove strongly and positively (+0.76 in CSA, +0.82 in PCA): firms that diversify operating-cash-flow deployment also diversify capital-market interactions. Both correlate negatively with the income-statement subgraph (−0.56 and −0.71 in CSA; −0.63 and −0.76 in PCA): when revenue, expense, and tax composition spreads more evenly across line items, the residual reorganization of balance-sheet and financing flows concentrates, and vice versa. The pattern is empirical, not an algebraic identity, but it surfaces only once the partition separates the value-creation channel from the capital-deployment and capital-market channels.

Second, total graph entropy correlates near zero with each subgraph entropy at the aggregate level under CSA (−0.02, +0.21, −0.02). This is not a measurement artifact: by Proposition 1, the three subgraph entropies aggregate into total entropy through a weighted sum plus the cross-subgraph weight entropy, and the partially offsetting movements among the three subgraphs leave the total only weakly correlated with any single component. This is the econometric counterpart of the decomposability property of Shannon entropy: the four filtered series $\mathcal{U}^{H^{\text{Tot}}}$, $\mathcal{U}^{H^{\text{OG}}}$, $\mathcal{U}^{H^{\text{IS}}}$, $\mathcal{U}^{H^{\text{FG}}}$ that emerge from the JLN filter applied to each input separately are not collinear restatements of a single underlying finding—they reflect the multi-dimensional structured uncertainty index of Section 3.4.

Third, the within-firm first-difference correlations in Panel C are small in magnitude across all subgraph pairs (medians $|\rho| < 0.05$), establishing that the four series do not duplicate each other at the level the JLN filter operates—namely, on within-firm fluctuations after the firm-specific persistent component is absorbed. Each subgraph carries information that cannot be inferred from the others. This is the empirical content of the structured-index claim: the filtered volatilities measure four economically distinct dimensions of firm uncertainty.

Common factor structure. The first principal component of the firm-level standardized entropy panel explains 18% of total variance for the total graph, 18% for the financing subgraph, 9% for the operating subgraph, and 38% for the income-statement subgraph. The first ten components together explain 66%, 52%, 49%, and 81% respectively. The income-statement subgraph carries the strongest common factor: revenue-cost-tax composition moves with macroeconomic conditions in ways shared across firms. The operating subgraph carries the weakest common factor: capital-deployment configuration is the most firm-specific of the structural margins. The PCA aggregation we report alongside CSA throughout Section 4.3 is therefore most informative when applied to income-statement entropy and least informative when applied to operating entropy—a finding consistent with the differential performance of the two aggregation schemes in the filter results.

Channel-specific dynamics around recessions. Table 20 reports lead-lag correlations between each entropy series and an NBER recession indicator. The pattern is striking and economically interpretable. Income-statement entropy $\bar{H}_t^{\mathrm{IS}}$ is strongly contemporaneously correlated with recessions (+0.37 at lag 0) and *leads* the cycle: its correlation with NBER peaks at +0.56 four quarters *before* the recession. Income-statement composition broadens before the formal contraction begins, as firms' realized revenue and cost shares spread across components in anticipation of demand and cost shocks. Operating-subgraph entropy moves in the opposite direction *after* recessions (−0.21 to −0.41 at lags two to four quarters before; +0.17 to +0.23 at lags one to three quarters after), reflecting concentration during contractions and re-diversification during recoveries. Financing-subgraph entropy is mildly counter-cyclical (−0.31 four quarters before recession), reflecting the contraction in the diversity of financing instruments firms use during downturns. Pairwise Granger-causality tests at lag 4 confirm the leading role of FG and IS entropy: $\bar{H}_t^{\mathrm{FG}}$ Granger-causes $\bar{H}_t^{\mathrm{OG}}$ ($F = 3.54$, $p = 0.011$), and $\bar{H}_t^{\mathrm{IS}}$ Granger-causes $\bar{H}_t^{\mathrm{OG}}$ ($F = 2.69$, $p = 0.038$).

The lead-lag structure has two implications. First, contrary to a common worry that backward-looking accounting measures lag economic conditions, the entropy series are *not* backward-looking in the relevant sense: the income-statement subgraph leads the cycle at horizons up to four quarters. This is because what enters the bookkeeping graph each quarter is the realized composition of value-creation flows, and composition responds to managerial expectations about demand and cost conditions before the level of profit shrinks mechanically. Second, the heterogeneous lead-lag structure across subgraphs licenses the structured-index attribution. A single index that lumped all four channels together would smooth out these distinct timings; the subgraph decomposition

Table 20: Lead-Lag Correlations with NBER Recession Indicator

	Entropy leads NBER					NBER leads entropy			
	-4	-3	-2	-1	0	$+1$	$+2$	$+3$	$+4$
$\bar{H}_t^{\text{Tot}}$	0.26	0.31	0.23	0.17	0.09	0.04	0.05	0.08	0.10
$\bar{H}_t^{\text{OG}}$	-0.41	-0.32	-0.21	-0.05	0.08	0.17	0.21	0.23	0.20
$\bar{H}_t^{\text{IS}}$	0.56	0.55	0.51	0.46	0.37	0.26	0.19	0.13	0.16
$\bar{H}_t^{\text{FG}}$	-0.31	-0.32	-0.25	-0.17	-0.11	-0.05	-0.05	-0.11	-0.17

Notes: Each cell is the Pearson correlation between the entropy series at time t and the NBER recession indicator at time $t+k$, where k is the column header. Negative k means entropy leads the NBER cycle; positive k means entropy lags. NBER recession quarters in the sample: 1990Q3–1991Q1, 2001Q1–2001Q4, 2007Q4–2009Q2.

preserves them.

Heteroskedasticity in the cross-section. A final property worth noting is heteroskedasticity in the cross-sectional dispersion of H_{it} across firms. The average within-quarter cross-sectional standard deviation of H_{it}^{IS} is 15% higher in NBER recession quarters ($\bar{\sigma}_{cs} = 0.091$) than in expansion quarters ($\bar{\sigma}_{cs} = 0.079$), and that of H_{it}^{FG} is 6% higher in recessions. The temporal variance of the cross-sectional mean $\bar{H}_t^{\text{IS}}$ is itself nearly four times as large in recessions as in expansions (Levene test $F = 11.65$, $p = 0.001$). Two forms of heteroskedasticity coexist: recessions widen the cross-section of structural states, and they elevate the time-series volatility of the cross-sectional mean. This is precisely the cross-sectional heterogeneity that JLN's factor-augmented Stage 1 is designed to absorb at the firm level before extracting the common volatility component, and the property that makes a factor-PC aggregation in Stage 2 informative.

Implications for the filter. The properties together establish that Accounting Graph Entropy is a suitable input class for the JLN filter. It is bounded, persistent, business-cycle-relevant, and exhibits conditional heteroskedasticity at the firm level. The subgraph decomposition of Proposition 1 extends these properties from a scalar to a vector of inputs, each inheriting the same profile through the additive structure of Shannon entropy. The economic interpretation of the resulting filtered series follows from Proposition 3 of Section 3.2: under rational expectations, the filtered conditional volatility of H_{it} reads the time-varying uncertainty about the unobserved economic state s_t that drives the firm's structural reorganization. The lead-lag and Granger results, the cross-channel correlations bounded away from one, and the order-of-magnitude differences in common-factor strength across subgraphs together suggest that the four filtered series will not be collinear restatements of a single underlying finding—a prediction that Sections 4.1–5.2 confirm and that the structured horse-race results in Section 5.3 exploit.[13]

[13] Accounting Graph Entropy is order-invariant on the adjacency matrix of G_{it}: permuting any pair of entries in the matrix leaves H_{it} unchanged (Liang et al., 2026). The measure therefore captures the distribution of edge weights but not the full topology of the bookkeeping graph—two graphs with identical edge-weight distributions but different connection patterns share the same AGE. For our purposes, this limitation is mild: the bookkeeping

D Channel-Specific Investment Regressions: Firm-Level Panel for ISG and FG

The body of the paper reports firm-level panel regressions for the total-graph and operating-subgraph Entropic Uncertainty Indices (Tables 5 and 6) and aggregate time-series regressions for all four channel-specific indices (Tables 7, 8, 9, and 10). For completeness, this appendix reports the firm-level panel regressions for the income-statement-subgraph and financing-subgraph EUIs.

Income-statement-subgraph EUI: firm-level panel. Table 21 reports the firm-level panel regressions with EUI^{ISG} as the regressor of interest. The pattern reveals the distinctive signature of the income-statement channel: EUI^{ISG} is statistically indistinguishable from zero in Panels A and B, which include both firm and time fixed effects, but enters with the theoretically predicted negative sign and marginal significance in Panels C and D, which include only firm fixed effects (so that the aggregate benchmarks EPU, VIX, JLN Macro, and JLN Financial are not absorbed by the time fixed effects). At $h = 1$, the Panel D coefficient is -0.0007 ($t = -2.64$). The differential between Panels A–B and Panels C–D is itself informative: it shows that the predictive content of EUI^{ISG} at the firm-quarter level operates almost entirely through cross-sectionally common variation, which is removed when time fixed effects are included. This is consistent with the aggregate-level result documented in Table 9, where EUI^{ISG} achieves $R^2 = 0.814$ in the full horse race and absorbs JLN Macro ($t = +1.57$): the income-statement channel reads aggregate macro-uncertainty rather than firm-specific structural variation.

Financing-subgraph EUI: firm-level panel. Table 22 reports the parallel result for the financing-subgraph EUI. EUI^{FG} is statistically indistinguishable from zero at every horizon and in every specification, with point estimates that are economically negligible (all $|t| < 1.4$). This pattern is the firm-level analogue of the comparatively weak aggregate financing-subgraph result in Table 10. Reorganization of the firm's capital-market interactions follows—rather than drives—the underlying structural reorganizations of operations and value-creation margins, and the resulting filtered conditional volatility carries correspondingly weaker predictive content for capital investment.

Synthesis of the four-channel firm-level evidence. Reading the firm-level panel evidence across all four channels together—Tables 5 and 6 in the body, and Tables 21 and 22 in this appendix—the channel hierarchy in firm-level predictive content for capital investment is unambiguous: EUI^{OG} is dominant (firm Panel D $h = 1$: $t = -7.51$), EUI^{tot} is strong ($t = -5.17$), EUI^{ISG}

graph's topology is itself disciplined by the three accounting laws of Section 2.1, and our object of interest is the time-series movement of H_{it}. Topological features of the bookkeeping graph beyond AGE—spectral measures based on the Laplacian, motif-based decompositions, and node-based classifications such as the ACE measure of Li et al. (2024)—are alternative summaries that complement AGE and that the broader agenda of Liang (2026) discusses.

Table 21: CAPX/Assets and EUI$^{\text{ISG}}$ — Firm-Level Panel

	Panel A				**Panel C**			
	$h=1$	$h=2$	$h=3$	$h=4$	$h=1$	$h=2$	$h=3$	$h=4$
EUI$^{\text{ISG}}$	−0.0003	−0.0003	−0.0003	−0.0002	−0.0008***	−0.0007***	−0.0007***	−0.0005**
	(−1.07)	(−1.05)	(−1.06)	(−0.76)	(−3.07)	(−2.85)	(−2.94)	(−2.50)
JLN Firm					−0.0004*	−0.0003*	−0.0003*	−0.0002
					(−1.74)	(−1.66)	(−1.71)	(−1.03)
EPU					−0.0006**	−0.0007***	−0.0004	−0.0008***
					(−2.47)	(−3.12)	(−1.50)	(−2.79)
VIX					0.0003	0.0002	−0.0000	0.0001
					(1.15)	(0.97)	(−0.08)	(0.58)
JLN Macro								
JLN Finance								
N	9,824	9,691	9,564	9,441	9,824	9,691	9,564	9,441
R^2	0.052	0.058	0.063	0.057	0.162	0.170	0.173	0.170
	Panel B				**Panel D**			
	$h=1$	$h=2$	$h=3$	$h=4$	$h=1$	$h=2$	$h=3$	$h=4$
EUI$^{\text{ISG}}$	−0.0002	−0.0002	−0.0002	−0.0001	−0.0007***	−0.0006**	−0.0006**	−0.0004**
	(−0.84)	(−0.80)	(−0.83)	(−0.57)	(−2.64)	(−2.40)	(−2.50)	(−2.03)
JLN Firm	−0.0004*	−0.0004*	−0.0004*	−0.0003	−0.0004*	−0.0003*	−0.0003	−0.0002
	(−1.77)	(−1.88)	(−1.70)	(−1.41)	(−1.82)	(−1.65)	(−1.59)	(−0.92)
EPU					−0.0005**	−0.0007***	−0.0003	−0.0007**
					(−2.35)	(−2.86)	(−1.11)	(−2.42)
VIX					0.0006**	0.0009***	0.0012***	0.0013***
					(2.33)	(3.94)	(4.78)	(4.62)
JLN Macro					−0.0007***	−0.0006***	−0.0005**	−0.0005**
					(−3.58)	(−3.06)	(−2.45)	(−2.44)
JLN Finance					0.0001	−0.0005*	−0.0011***	−0.0011***
					(0.38)	(−1.74)	(−4.09)	(−3.76)
N	9,824	9,691	9,564	9,441	9,824	9,691	9,564	9,441
R^2	0.054	0.060	0.065	0.058	0.165	0.173	0.179	0.176
Firm Controls	Yes				Yes			
Fixed Effects	Firm + Time [a]				Firm [b]			

Notes: EUI$^{\text{ISG}}$ is the income-statement-subgraph Entropic Uncertainty Index (standardized). Dependent variable is CAPX/Assets (h quarters ahead). Uncertainty measures are standardized (mean 0, s.d. 1). t-statistics in parentheses. *** $|t| \geq 2.576$; ** $|t| \geq 1.960$; * $|t| \geq 1.645$.

[a] Panels A and B: firm and time FE. [b] Panels C and D: firm FE only (aggregate benchmarks absorbed by time FE). Standard errors clustered by firm.

Table 22: CAPX/Assets and EUI^{FG} — Firm-Level Panel

	Panel A				**Panel C**			
	$h=1$	$h=2$	$h=3$	$h=4$	$h=1$	$h=2$	$h=3$	$h=4$
EUI^{FG}	−0.0001	−0.0000	−0.0001	0.0000	−0.0002	−0.0001	−0.0002	−0.0001
	(−0.64)	(−0.23)	(−0.32)	(0.04)	(−1.26)	(−0.66)	(−0.81)	(−0.38)
JLN Firm					−0.0004**	−0.0004**	−0.0004**	−0.0003
					(−2.09)	(−1.99)	(−2.02)	(−1.30)
EPU					−0.0006***	−0.0008***	−0.0004*	−0.0008***
					(−2.71)	(−3.33)	(−1.67)	(−2.91)
VIX					0.0002	0.0002	−0.0001	0.0001
					(1.00)	(0.83)	(−0.22)	(0.45)
JLN Macro								
JLN Finance								
N	9,824	9,691	9,564	9,441	9,824	9,691	9,564	9,441
R^2	0.052	0.058	0.063	0.057	0.158	0.167	0.170	0.168
	Panel B				**Panel D**			
	$h=1$	$h=2$	$h=3$	$h=4$	$h=1$	$h=2$	$h=3$	$h=4$
EUI^{FG}	−0.0001	−0.0000	−0.0001	0.0000	−0.0003	−0.0001	−0.0002	−0.0001
	(−0.60)	(−0.19)	(−0.28)	(0.06)	(−1.36)	(−0.73)	(−0.82)	(−0.39)
JLN Firm	−0.0004*	−0.0004**	−0.0004*	−0.0003	−0.0004**	−0.0004*	−0.0004*	−0.0002
	(−1.88)	(−1.99)	(−1.80)	(−1.48)	(−2.12)	(−1.94)	(−1.86)	(−1.14)
EPU					−0.0006**	−0.0007***	−0.0003	−0.0007**
					(−2.51)	(−3.01)	(−1.21)	(−2.45)
VIX					0.0006**	0.0009***	0.0012***	0.0013***
					(2.33)	(3.92)	(4.70)	(4.55)
JLN Macro					−0.0009***	−0.0008***	−0.0006***	−0.0006***
					(−4.31)	(−3.72)	(−3.11)	(−2.92)
JLN Finance					0.0002	−0.0004	−0.0011***	−0.0011***
					(0.59)	(−1.57)	(−3.92)	(−3.61)
N	9,824	9,691	9,564	9,441	9,824	9,691	9,564	9,441
R^2	0.053	0.060	0.064	0.058	0.162	0.171	0.177	0.175
Firm Controls	Yes				Yes			
Fixed Effects	Firm + Time [a]				Firm [b]			

Notes: EUI^{FG} is the financing-subgraph Entropic Uncertainty Index (standardized). Dependent variable is CAPX/Assets (h quarters ahead). Uncertainty measures are standardized (mean 0, s.d. 1). t-statistics in parentheses. *** $|t| \geq 2.576$; ** $|t| \geq 1.960$; * $|t| \geq 1.645$.
[a] Panels A and B: firm and time FE. [b] Panels C and D: firm FE only (aggregate benchmarks absorbed by time FE). Standard errors clustered by firm.

is marginal ($t = -2.64$), and EUI^{FG} is null ($t = -1.36$). The contrast with the aggregate-level rankings of Tables 8 and 9—in which EUI^{ISG} achieves aggregate $R^2 = 0.786$, comparable to EUI^{OG}'s 0.777—is the structural-economic content of the channel decomposition: the operating channel reads firm-specific capital-deployment uncertainty, the income-statement channel reads aggregate value-creation uncertainty, and the financing channel reads downstream reorganization. Only an exact, theory-grounded subgraph decomposition—of the kind Proposition 1 delivers—can isolate these distinct economic readings from a single estimator.